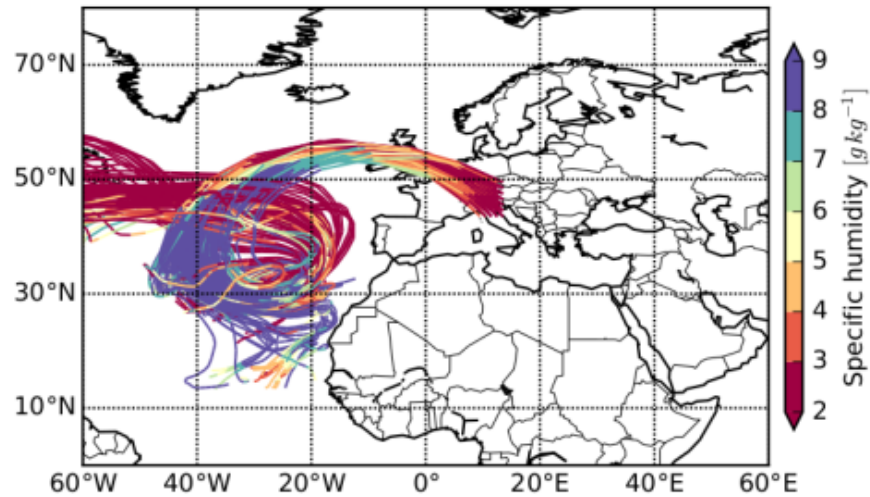# Heavy precipitation and flood

Final Report
April 2016

Institute for Atmospheric and Climate Science, ETH Zurich
Institute of Environmental Engineering, ETH Zurich
Hybest GmbH

Commissioned by the Federal Office for the Environment (FOEN)

Figures title page

Top image: 10-day trajectories (colored with specific humidity) illustrating moisture transport contributing to the December 1991 floods in Switzerland,
Bottom image: flood in the Schächen in 1910, seen from the Schattdorf bridge.

Table of content

Introduction

1.1 The problem

Design floods for river protection works are usually based on the magnitude of rare floods. The 100-year flood was mainly used for this purpose until the end of the last century. After the devastating 1987 floods, it was realized that the protection objectives should be differentiated (BAFU, 2001). Therefore, also the magnitudes of the HQ300, EHQ, HQ1000, and PMF became important. However, already the 100-year flood can only be estimated with large error margins. The uncertainty has even increased, because catchments experienced several floods in the last decades that were defined before as 100 year floods.

Floods with defined return periods are estimated using statistically analyzed discharge time series (Fig. 1.1). Several problems are associated with this approach:

As discharge series are rarely longer than 90 years, statistical extrapolations have to be used. They are based on grossly simplified assumptions, mirroring only an average behavior. They cannot account for the individual catchments characteristic. Observed floods often exceed the large associated confidence intervals (Fig. 1.2). They are called outliers. Despite an extensive literature, there is no accepted rule how to incorporate the influence of such outliers on statistical flood measures.

Consideration of historical floods is a powerful tool to enhance conventional analyses. Under favorable circumstances, the data base can be extended by several centuries. However, the accuracy is limited and no insight into the specific reaction of a catchment under changed boundary conditions is possible.

Hydrological models, fed with extrapolated meteorological inputs, can be used to study flood behavior in the extrapolation range. As rivers react vastly differently to differences in meteorological input and in the way runoff is formed (Fig. 1.1), these models have to be calibrated with precipitation and discharge records. However, a successful calibration does not guarantee that model results are also valid in the extrapolation range. This is only the case, if the model correctly reproduces the behavior of the relevant runoff processes with increasing precipitation.

Another critical point, usually not discussed in detail, is the extrapolation of the meteorological input. Just transferring values from nearby stations or statistically extrapolating some station data, as it is usually done, is inadequate for these complex processes.

Several of these critical points are addressed in the following chapters.
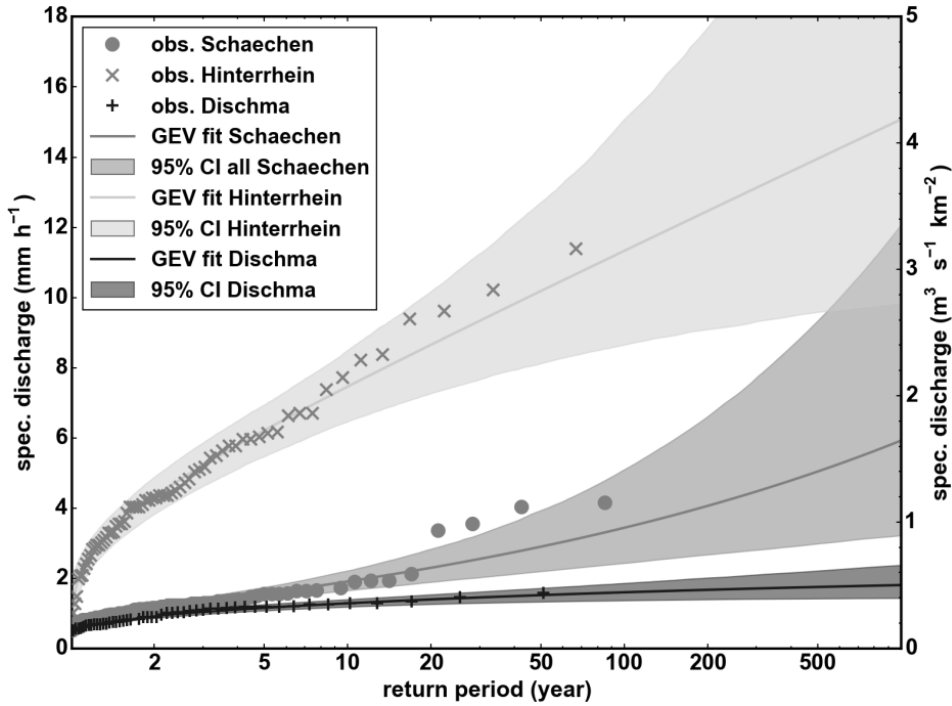
Figure 1.1: Flood frequency analysis of the Hinterrhein, Schächen and Dischma catchments. Generalized Extreme Value (GEV) distributions were fitted to the yearly maximum floods record. The 95% confidence intervals (CI) were estimated from a parametric bootstrap procedure with 2000 draws.
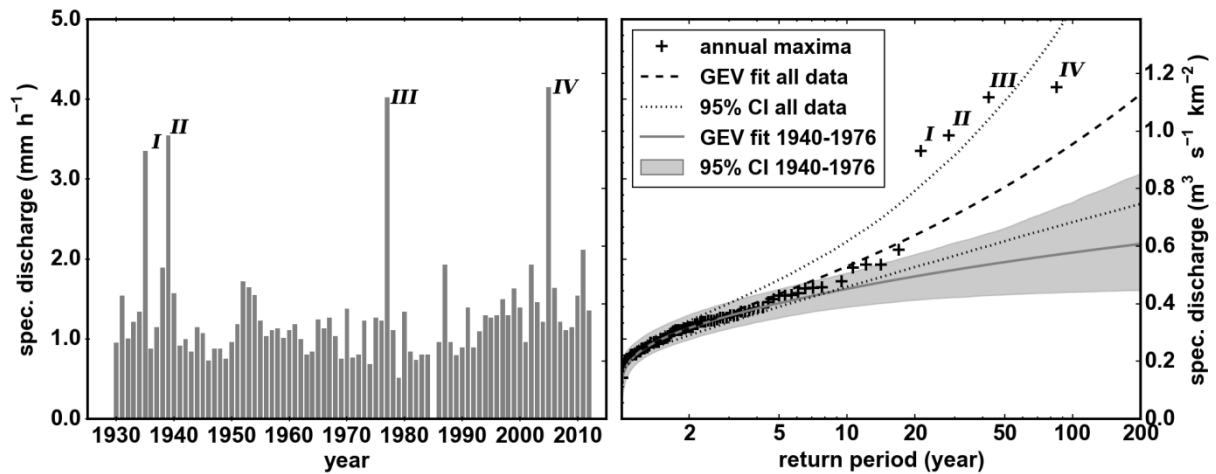
Figure 1.2: Flood frequency analysis of the Schächen in Bürglen. a) Yearly maximum floods. b) Return periods of different flood magnitudes with fitted General Extreme Value (GEV) distributions. The 95% confidence intervals (CI) were estimated from a parametric bootstrap procedure with 2000 draws. Note the apparent step-change around a return period of 20 years, caused by the four remarkably large floods (indicated with Roman numerals).

5

1.2 Project description

In the last decades, progress in meteorological and hydrological simulations has been considerable, mainly due to improved knowledge of relevant processes and the enormously increased computing power. In this project, new techniques have been combined to assess their potential to improve flood estimation in the extrapolation range.

Table 1.1 gives an overview on large precipitation events in Switzerland since 1910 and the resulting floods in some well-studied catchments. Highlighted are events that were selected for extensive COSMO-2 simulations in this project. Figure 1.3 shows the catchments that are specifically considered in this project.
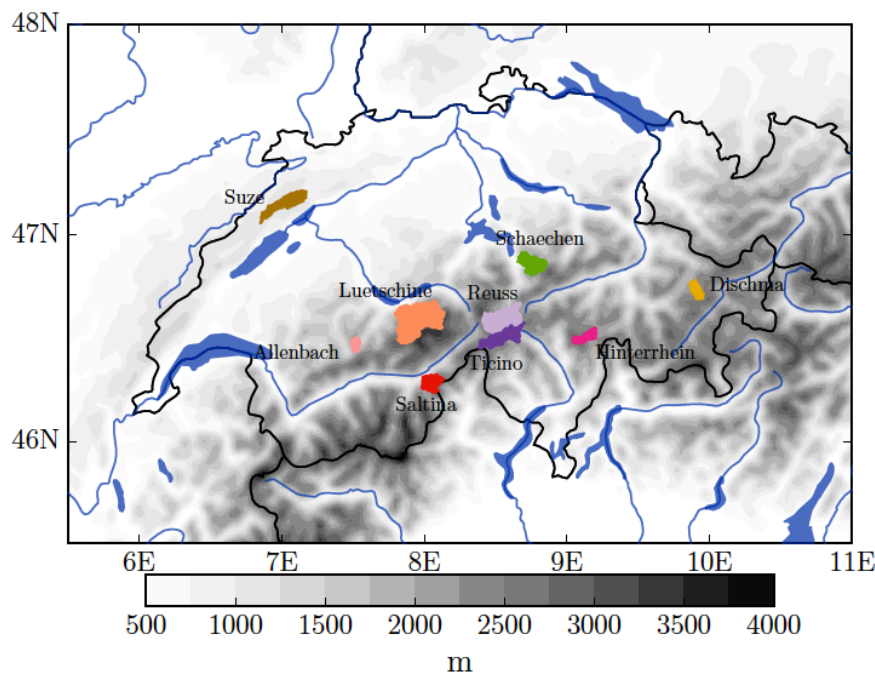
Figure 1.3: The considered catchments in Switzerland (colored polygons). The grey shading shows the topography in m.

Chapter 2 covers the meteorological techniques and results. In chapter 2.1 weather situations leading to heavy precipitation are classified using moisture uptake and transport patterns obtained from air parcel trajectories. In chapter 2.2, results of COSMO-2 simulations are presented. It is qualitatively assessed, how well precipitation distributions of the events indicated in Table 1.1 could be reproduced in the COSMO-2 control simulations. Then, sensitivity experiments are introduced, for which boundary conditions of humidity and temperature have been increased. The intention was to maximize extreme events under realistic flow conditions. The effects of these changes on the precipitation fields, amounts and intensities are analyzed. In chapter 4 the results from the COSMO-2 simulations are used in the hydrologic model Qarea+ (Chapter 3) to extrapolate to extremer floods.

As research after the 2005 flood showed, runoff formation and peak flow in steep alpine catchments depend heavily on the extent of landforms with large storage capacities, such as moraines, debris cones, moving landmasses, etc. Chapter 3 details how the hydrologic model Qarea+ considers these influences. The effect is demonstrated with simulations in different catchments.

In the first part of Chapter 4, Qarea+ simulations using synthetic rains with increasing volumes and intensities are applied to the Schächen, Hinterrhein and Dischma catchment. In this way, the effect of different compositions of delayed reacting landforms on flood magnitude becomes visible, as well as their influence on the extrapolation. In the second part, maximized COSMO-2 results are used as input to the Qarea+ model. The adopted rainfalls and therefore the resulting discharges are physically plausible. However, their very high return period cannot yet be properly assessed, due to a lack of a proper statistical assessment, which would require much longer meteorological time series.

In the last chapter, the results and their practical application are discussed.

Date	wind direction	moisture source region type	Schaechen (Buerglen) 108 m³s⁻¹	mmh⁻¹	RP	Hinterrhein (Hinterrhein) 54.2 m³s⁻¹	mmh⁻¹	RP	Dischma (Kriegsmatte) 43.3 m³s⁻¹	mmh⁻¹	RP	Weisse Luetschine (Zweiluetschinen) 165 m³s⁻¹	mmh⁻¹	RP	Luetschine (Gsteig) 381 m³s⁻¹	mmh⁻¹	RP	Saltina (Brig) 76.5 m³s⁻¹	mmh⁻¹	RP	Suze (Sonceboz) 130 m³s⁻¹	mmh⁻¹	RP	Reuss (Andermatt) 190 m³s⁻¹	mmh⁻¹	RP	Ticino (Piotta) 159 m³s⁻¹	mmh⁻¹	RP	Emme (Eggiwil) 124 m³s⁻¹	mmh⁻¹	RP
Events simulated with COSMO-2																																	
18-Jul-1987	SW	south-west	29	1.0	<2	167	11.1	100	15.2	1.3	8	45	1.0	<2	nF	nF	nF	16	0.8	<2			0	149	2.8	8	53	1.2	4	nF	nF	nF
24-Aug-1987	S-SW	south(-east)	54	1.8	8	38	2.5	<2	14.6	1.2	7	69	1.5	3	133	1.3	3	42	2.0	8			0	289	5.5	100	213	4.8	>100	78	2.3	<2
20-Aug-1988	S	south-west	15	0.5	<2	149	9.9	50	nF	nF	nF	50	1.1	<2	93	0.9	<2	11	0.5	<2			0	25	0.5	<2		0.0		nF	nF	nF
22-Dec-1991	NW	north-west	27	0.9	<2	nF	nF	nF	nF	nF	nF	21	0.5	<2	80	0.8	<2	7	0.3	<2	65	1.8	150	nF	nF	nF				95	2.8	2
24-Sep-1993	S-SE	south(-east)	nF	nF	nF	54	3.6	<2	nF	nF	nF	57	1.2	<2	129	1.2	2	99	4.7	50			0	172	3.3	10	78	1.8	6	24.7	0.7	<2
15-Oct-2000	S-SE	south(-east)	nF	nF	nF	26	1.7	<2	nF	nF	nF	81	1.8	10	186	1.8	30	125	5.9	100			0	156	3.0	9	70	1.6	5	24	0.7	<2
12-Aug-2002	NE	mix	56	1.9	9	nF	nF	nF	6.7	0.6	<2	82	1.8	10	179	1.7	25	nF	nF	nF			0	21	0.4	<2		0.0		115	3.3	3
22-Aug-2005	(NE-NW)	north-east	125	4.2	100	nF	nF	nF	17.5	1.5	30	108	2.4	50	254	2.4	300	nF	nF	nF			0	31	0.6	<2				178	5.2	18
08-Aug-2007	SW	mix	35	1.2	<2	16	1.1	<2	3.8	0.3	<2	77	1.7	6	210	2.0	70	13	0.6	<2	50.5	1.4	30	44	0.8	<2		0.0		176	5.1	18
10-Oct-2011	NW?	north-west	60	2.0	10	nF	nF	nF	4.5	0.4	<2	111	2.4	70	226	2.1	100	4.4	0.2	<2			0	37	0.7	<2		0.0		106	3.1	2
01-Jun-2013		north-east																														
Relevant other events																																	
14/15-Jun-1910	NE-N		130	4.3	100																											
23-Sep-1920	SE																															
25-Sep-1927	SW																															
30-Oct-1935	NW?																															
05-Aug-1939	S?																															
24-Nov-1944	N?																															
31-Jul-1977	NE																															
08-Aug-1978	SW																															
15-Jun-1987									14.7	1.2	6	82	1.8	10																		
03-Jul-1987									14.8	1.2	6																					
25-Sep-1987																																
16-Feb-1990																																
12-May-1999																																
22-May-1999			48 / 35	1.6 / 1.2	7	18	1.2	<2	8 / 16	0.7 / 1.3	<2 / 13																					
03-Jun-1999									12.3	1.0	4																					
21-Sep-1999									13	1.1	5															62	1.8	5			
26-Sep-1999			nF	nF	nF	137	9.1	30																			26	1.8	<2			
05-Jun-2002																											70	1.8	6			
16-Nov-2002			58	1.9	10	121	8.0	15																								
29-Aug-2003			nF	nF	nF																											
24-Aug-2004												76	1.7	6																		
02-Nov-2004																		52	1.8	10												
17-Sep-2006			48	1.6	7	13	1.6	<2	nF	nF	nF																					
03-Oct-2006			nF	nF	nF	143	9.5	50	nF	nF	nF																					
29-May-2008																		61	1.8	15												
13-Jul-2008			30	1.0		48	3.2	<2	13.8	1.1	6																77	1.8	7			
06-Sep-2008																																

Table 1.1: Large floods in Switzerland since 1910 that were considered in the project, with the corresponding flood peak magnitudes with their return periods (RP) for selected catchments. Events that produced runoff peaks smaller than the smallest yearly maximum are listed as ' nF' (no flood). The governing wind direction and moisture source diagnostic are also listed. Red text indicates that the event could not be adequately reconstructed with COSMO-2, the largest events of which are marked with a green background shading. Orange shading indicates that an event is of particular interest. Catchment-event combinations for which the flood records were not studied are kept blank.

2 Meteorology

2.1 Characterization of weather situations leading to heavy precipitation using a trajectory-based moisture source diagnostic

2.1.1 Methods

Weather classifications

Weather changes from day to day, but certain flow patterns appear to repeat themselves. Therefore, already decades ago, different approaches have been developed for classifying weather situations into certain „weather classes" or „weather types". Traditional approaches, for instance from Hess and Brezowsky (Gerstengarbe and Werner 1999) and Schüepp (1959; 1996) are based mainly on a subjective analysis of the instantaneous flow in a predefined region. From 2004-2010, the EU funded COST action 733 (cost733.met.no) had the objective to develop a general method for assessing, comparing and classifying weather situations in Europe (Huth et al. 2008). Also these methods, although automated and more objective, relied on the flow field at a given time. The disadvantage of these approaches is that they do not consider the time integrated flow evolution, e.g., the flow over Switzerland might be from the west at a given time, but this does not necessarily imply that air from the North Atlantic is advected because the air might originate south of the Alps and then arrive in Switzerland as part of a cyclonic circulation along a curved path from the west.

A method based on moisture sources for heavy precipitation

Therefore, in this project, we decided to implement an alternative approach, which considers the time history of the air parcels arriving in Switzerland. Ramos et al. (2014) proposed a first version of such a trajectory-based weather classification. Here, instead, we decided to not do a categorical categorization but to rather develop a method that allow characterizing the flow conditions leading to extreme precipitation events in Switzerland in a meaningful way. Our approach characterizes weather situations by tracking from which ocean and land regions the moisture transported to Switzerland was evaporated. These so-called "moisture sources" can vary strongly from one event to another, as found in previous case studies (e.g., Winschall et al. 2014). Using the technique of Sodemann et al. (2008), we can identify and map for each precipitation event in Switzerland where the precipitated moisture evaporated during the previous 10 days (see example in Fig. 2.1). Technically, the method is based on 10-day backward trajectories from every grid point in the target region (here Switzerland) and an analysis of the moisture changes along these trajectories. For every 6-hourly time interval along the trajectories it is checked whether moisture increases; if yes then this moisture increase in the air parcel is attributed to surface evaporation. In this way, by evaluating hundreds of trajectories per day, it is possible to construct a two-dimensional moisture source map as shown in Fig. 2.1. We applied this technique at 6-hour intervals to both the ERA-Interim (1979-2012; Dee et al. 2011) and 20CR reanalysis datasets (1871-2012; Compo et al. 2011). However, later when analyzing the results, we decided that the 20CR results are not fully reliable because of quality issues with the 20CR wind fields.

In a second step, we can then calculate averaged moisture source maps (so-called composites) for selected flood events in a specific catchment. For instance, the averaged moisture source map for the top 5 flood events of the Saltina can be compared to the map for the top 5 events of the Hinterrhein. Such a comparison shows whether moisture sources and moisture transport differ for extreme floods in different catchments.
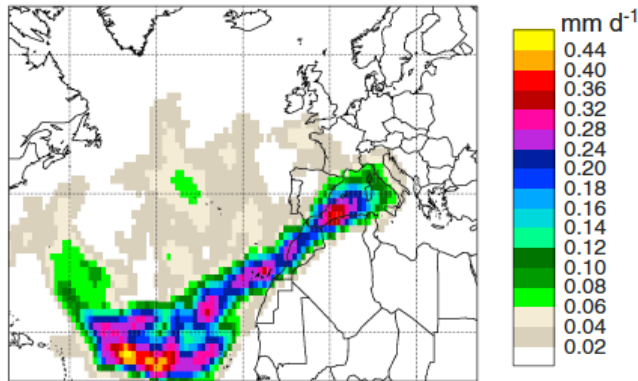

Figure 2.1: Example of the moisture source region for a heavy precipitation event in the western Mediterranean on 19 December 1996. The values show surface evaporation in mm per day. From Winschall et al. (2014).

2.1.2 Results and discussion

Moisture source patterns for flood events in selected catchments

As described in Section 2.1.1, moisture source composite maps have been produced for the most remarkable flood events since 1979 in 40 catchments in Switzerland. For a selection of catchments – the selection has been made to reveal the interesting variability of moisture source patterns between catchments – the results (for the top 5 events in the period from 1979 to 2011) are presented in Fig. 2.2 and briefly discussed here, going from southern, to western, to eastern Switzerland. The events used for the composites are listed in Table 2.1.

	Dischma	Emme	Hinterrhein	Luetschine	Saltina	Suze
Top 1	2005-08-23	1997-06-12	1987-07-18	2005-08-22	2000-10-15	1991-12-22
Top 2	1999-06-03	2005-08-22	1988-08-20	2007-08-08	2002-11-16	1990-02-14
Top 3	1987-07-18	2007-08-08	2006-10-03	2000-10-15	2008-05-29	2007-08-09
Top 4	1985-08-06	2008-07-30	1999-09-26	2002-08-12	2004-11-02	1999-02-22
Top 5	1997-06-29	2010-07-12	2003-08-29	1982-07-31	1987-08-25	1987-09-26

Table 2.1: Top 5 events for the period from 1979 to 2011 for the catchments used in Fig. 2.2. Events highlighted in blue were simulated in the scope of this project with the COSMO model.

Saltina (Fig. 2.2a): Moisture sources have a pronounced maximum in the Central Mediterranean between Italy and Tunisia, indicating that the Mediterranean is an important moisture source of heavy precipitation in the Saltina and that these events typically occur with southerly flow conditions. The large spread indicates, however, that also continental moisture sources contribute, especially from Western Europe and Northern Africa. Note that the composite map does not indicate that the moisture

sources are identical for the five events. The map represents an average over all events, which we regard as characteristic for extreme events in this particular catchment. Nevertheless substantial case-to-case variability is possible between individual cases. This remark is also valid for the other catchments.

Hinterrhein (Fig. 2.2b): Here the moisture source pattern has again almost no contributions from east of Switzerland, but strong contributions from Western Europe, the western Mediterranean, and from the North Atlantic, reaching to beyond 60°W. Such a pattern is consistent with prominent upper-level troughs, which propagate fairly rapidly over Europe, in contrast to more stationary cutoff situations. Typical rainfall associated with strong troughs is intense, accompanied by the passage of fronts, and often of relatively short duration (less than one day). It is therefore very interesting to see that the hydrologically fast-responding Hinterrhein catchment experiences floods under such flow conditions, whereas slower reacting catchments (e.g., Dischma, Lütschine) require a cutoff situation to experience floods. In other words that Hinterrhein is more sensitive to intensity and Dischma to the duration of the precipitation event.

Suze (Fig. 2.2c): This is the most westward extending moisture source pattern reaching beyond 60°W and covering latitudes between 20 and 60°N. Peak values occur in the central North Atlantic west of the Azores, indicating a prominent role of remote moisture sources and large-scale moisture transport. Mediterranean moisture sources are almost absent and continental contributions are comparatively weak. Such an uptake pattern is consistent with a situation where moisture is advected around a high-pressure system in the eastern North Atlantic from the Northwest towards the Jura (cf. Piaget et al., 2015). Meteorologists also often refer to these long-range moisture transport patterns as "atmospheric rivers" (e.g., Stohl et al. 2008).

Lütschine (Fig. 2.2d) and Emme (Fig. 2.2e): The moisture source patterns for these two catchments are fairly similar. They show high values in a large area extending from Western to Eastern Europe, with peak values in the western Alps. For the Lütschine, there is also a significant contribution from Central Mediterranean. The large-scale patterns for Lütschine and Emme indicate a high case-to-case variability of moisture sources and transport patterns associated with extreme precipitation in these regions. Therefore, the moisture pathway for the October 2011 Lütschine event, discussed by Piaget et al. (2015) is not representative for all flood events in this catchment.

Dischma (Fig. 2.2f): A similarly broad pattern emerges for the Dischma composite with moisture uptakes reaching very far west to almost 60°W (Newfoundland) but also far east to 40°E (Russia). The far eastern moisture sources that occur for floods in the Lütschine, Emme and Dischma catchments are remarkable because they indicate that moisture is transported during these events against the mean westerly flow. Such behavior was also observed for the June 2013 Danube and Elbe flood (Grams et al. 2014) and it typically occurs in situations with a quasi-stationary upper-level cutoff located over Central Europe.
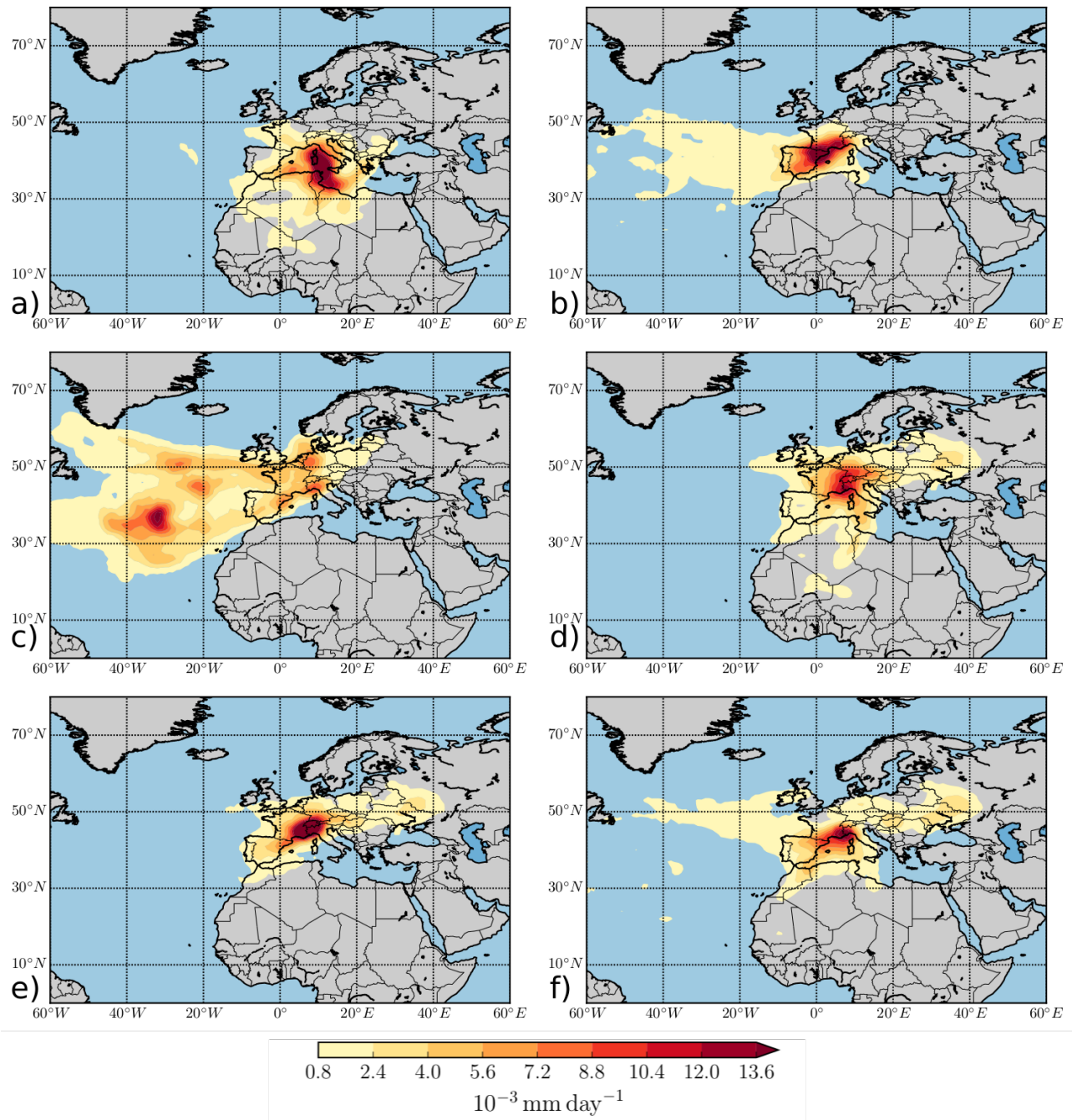
Figure 2.2: Moisture source uptake composites (averages) (in mm per day) for the top 5 flood events since 1979 in the following catchments: a) Saltina, b) Hinterrhein, c) La Suze, d) Lütschine, e) Emme, and f) Dischma. The event dates used for the composites are listed in Table 2.1.

In summary, this analysis of moisture source patterns leads to the following interesting findings:

1) Moisture sources for flood events in Switzerland extend over a large domain, including the North Atlantic, Europe (south of 60°N), the western and central Mediterranean, and for some events parts of northern Africa.

2) Moisture sources of flood events vary between different catchments. They are mainly continental (reaching for into Eastern Europe) for Lütschine, Emme and Dischma, they are essentially from the west (with strong contributions from the North Atlantic) for La Suze and Hinterrhein (i.e., for catchments in very different parts of Switzerland!), and they are predominantly from the south for Saltina.

3) The patterns can be subjectively classified into four flow situations as presented in Fig. 2.3:

- Class 1 (Fig. 2.3a): Moisture transport around a stationary high-pressure system in the eastern North Atlantic (associated with North Atlantic moisture sources, potentially extending far in the subtropics); e.g., December 1991, October 2011.
- Class 2 (Fig. 2.3b): Quasi-stationary cutoff lows over Central Europe, i.e., close the Alps (associated with continental moisture sources extending into Eastern Europe); e.g., August 2005.
- Class 3 (Fig. 2.3c): Broad troughs moving from the North Atlantic across Europe (associated with moisture sources over the North Atlantic and western Europe); e.g., July 1987.
- Class 4 (Fig. 2.3d): Narrow troughs that are less stationary than the cutoffs but more than the broader troughs. They lead to very intense southerly winds towards the Alps (associated with southern moisture sources over the Mediterranean and northern Africa); e.g., September 1993, October 2000.
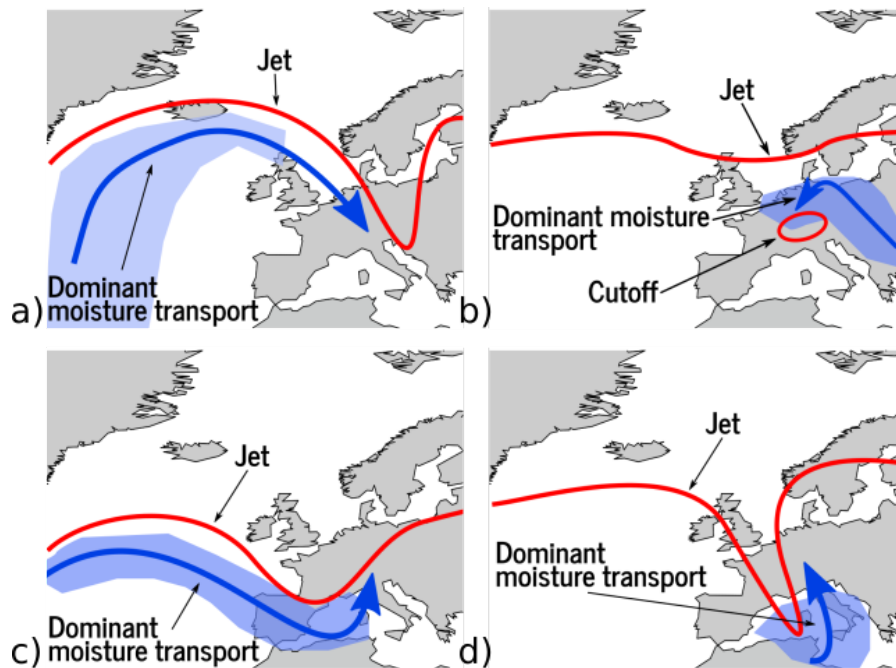

Figure 2.3: Schematics of the four main meteorological situations leading to floods in Switzerland. a) Class 1, b) Class 2, c) Class 3, and d) Class 4 (see the text for details on the classes). The red lines show the position of the jet stream (at the level of the tropopause, i.e., at a height of about 10 km). The blue arrows show the dominant moisture transport and the blue areas mark the typical area of moisture uptake due to surface evaporation.

These classes can be compared with the previous classification by Stucki et al. (2012). Their pivoting cutoff (PVO) class is similar to our quasi-stationary cutoff scenario (Class 2), for example both contain the August 2005 event. Their elongated cutoff (ECO) is very similar to our narrow troughs category (Class 4), with the dominant moisture transport occurring from the western Mediterranean towards the Alps. In addition, their zonal flow (ZOF) class shares some characteristics with our Class 1 scenario with the stationary high-pressure system over the eastern North Atlantic, leading to a dominant moisture transport from the North Atlantic (or potentially from the Subtropics) driven by a strong westerly to north-westerly flow.

2.2 Sensitivity experiments with the COSMO-2 model

2.2.1 Methods

The convection-resolving model COSMO-2

Assuming that accurate initial and boundary conditions are available, then today's high-resolution regional weather prediction models are capable of realistically simulating the meteorological conditions leading to flood-producing Alpine precipitation events. This has been shown for instance by Hohenegger et al. (2008) for the August 2005 flood event in Switzerland and Davolio et al. (2015) for two autumn 2011 flood events in Liguria (Italy). These models have typically a grid spacing of 1-3 km, which allows (i) a so-called explicit treatment of deep convective clouds, and (ii) a fairly realistic representation of the Alpine topography. Both these aspects are essential for accurately simulating extreme precipitation events because:

- Extreme precipitation occurs typically in situations when a conditionally unstable temperature profile permits the formation of deep convective clouds and thunderstorms. Convective clouds are characterized by very strong updrafts (vertical winds up to 10 ms^{-1}) from the boundary layer to the upper troposphere (10-12 km), by the formation of large rain drops, graupel and in some cases hail, and by intense near-surface gust fronts, which can trigger new convective cells. These clouds are typically small, with a horizontal dimension of at most a few kilometers, and therefore until very recently weather prediction and climate models (with resolutions of 10-100 km) have not been able to explicitly resolve the dynamics of convective clouds. Instead, they used a so-called parameterization of deep convection, which in a statistically meaningful way tried to represent the net effect of deep convection on the larger-scale averaged grid point values of, e.g., temperature and humidity. These models have major shortcomings, for instance, in representing the diurnal cycle of summertime convection (e.g., Paulat et al. 2008; Dirmeyer et al. 2012) and the peak intensity of precipitation (e.g., Frei et al. 2003). With the latest generation of numerical weather prediction models (e.g., COSMO-2 at MeteoSwiss), parameterization of deep convection is no longer necessary and this cloud type can be simulated explicitly, i.e., in a physically much more consistent way. Therefore, these models are often referred to as "convection-resolving" (or "convection-permitting") models. The transition from models with parameterized to explicit convection can be regarded as a breakthrough in simulating extreme precipitation events (e.g., Ban et al. 2014).

COSMO-2, the model used in this project to perform sensitivity experiments belongs to this category of convection-resolving models.

- Topography plays an essential role for the formation of clouds and precipitation in Switzerland. Mountains distort the synoptic-scale flow and force air parcels to either flow around or flow over them, depending mainly on mountains height, static stability and flow speed (e.g., Klijun et al. 2001; Rotunno and Houze 2007). In the first case a stagnation point and flow splitting occurs on the windward side of a mountain, leading to strong precipitation mainly in the Alpine foreland. In contrast, in the second case moist air parcels traverse the Alpine crest, often resulting in the formation of convective clouds and heavy precipitation in the central Alps. Inner Alpine valleys and topographic gaps can lead to substantial variability in the airflow and resulting precipitation pattern. A fully realistic representation of the steepness and variability of Alpine topography in numerical weather prediction models is not yet possible. However, current models like COSMO-2 clearly have a much better representation of the most important Alpine features than earlier model generations, which significantly underestimated the height of mountains peaks and variability. Consequently, current models can produce a more accurate flow structure, triggering of convective cells and precipitation patterns.

However, despite this enormous improvement in the model representation of key meteorological processes that can lead to extreme precipitation events, simulating such events remains challenging and, for certain cases, still produces precipitation fields that differ considerably from reality. Some important reasons for this behaviour are: (i) initial and boundary conditions are inaccurate due to measurement errors and the scarcity of observations in regions with complex topography; (ii) the nature of the atmospheric flow is chaotic, i.e., small errors in the initial conditions can lead to large errors in the model simulations on the time scale of hours to a few days; and (iii) cloud microphysical processes, e.g., the growth of tiny cloud droplets to rain drops and the freezing of supercooled cloud droplets to snow crystals, can only be implemented in numerical models in simplified ways. This cautionary remark is important for this project because it implies that even when performing simulations of recent flood events with a state-of-the-art model and with greatest care, these simulations are always associated with errors and can only provide a sophisticated approximation of reality.

Rationale for the sensitivity experiments

As mentioned in the introduction, a central objective of this project has been to address the question, whether it is conceivable that in the coming decades flood events significantly exceed the intensity of recent extreme events (e.g., September 1993, October 2000, August 2005). If the answer was "yes", then the follow-up questions would be: (i) which catchments are most likely to experience larger floods than known until now, (ii) during what type of meteorological conditions would this occur, and (iii) what processes would lead to the increased magnitude of the extremes. These are extremely challenging questions and there are different options to approach them with the aid of numerical models:

- Regional climate change scenario simulations (e.g., Gobiet et al. 2014; Kotlarski et al. 2014; see also the Swiss Climate Change Scenarios CH2011: ch2011.ch). This approach considers the full chain from

estimates of global emission scenarios of greenhouse gases, to simulations of the global Earth System including interactions between the ocean, atmosphere and land, to simulations of the regional climate with nested higher-resolution models. A major advantage of this approach is that it can capture potential large-scale changes in the atmospheric circulation and their effects on the regional climate (e.g., a shift in the North Atlantic storm track with consequences for the frequency of frontal systems hitting the Alps). However, this "gold standard" approach is computationally very expensive and until today, robust multi-model multi-member ensemble simulations (IPCC 2013) are only feasible with models that are coarser than the aforementioned convection-resolving models and therefore potentially suffer from inadequacies in the representation of orographic heavy precipitation events. Also, in most studies of this kind, the focus of the analysis has been either on longer-time (e.g., seasonal) mean precipitation or on a statistical investigation of local extreme values, but rarely on the scale of individual events, which can strongly vary in space and time from one event to another.

- Surrogate climate change simulations (e.g., Schär et al. 1996; Kröner et al. 2016). This simpler methodology only requires a regional climate model and the key idea is that while the large-scale circulation is assumed to remain unaltered, the thermodynamics of climate change can be approximated by an increase of temperature at the model boundaries and an increase of specific humidity such that relative humidity remains constant. This approach is dynamically consistent but should be regarded as an idealized experiment. It is attractive because of the overall much smaller computational costs and the elegant design of the experiment, which allows assessing the thermodynamic effects of global warming in isolation. However, as for the real climate change experiments (see above), for computational reasons so far no surrogate climate change simulations are available with convection-resolving models.

- Case study sensitivity experiments with a convection-resolving model. As explained above, the rationale in this study is that in order to capture the essential processes leading to extreme precipitation events we should use a convection-resolving model. In this project this is the COSMO-2 model, which is also used currently by MeteoSwiss and other national weather services for operational weather forecasting. This model is first used to perform "realistic" simulations (representing the actual conditions) for a selection of events. In addition, inspired by the surrogate-climate change simulations mentioned before, sensitivity experiments with modified initial and boundary conditions are performed. The modifications concern either the temperature field (which is uniformly changed by 1 or 2°C) or the relative humidity field (which is uniformly changed by 10-30% as long as relative humidity does not exceed 100%). This allows addressing the following question: For a given heavy precipitation event, how would the precipitation field change if temperature or humidity had been increased but the initial flow conditions remained unchanged? It is important to note that this cannot be regarded as a proper climate change experiment, because of the assumption that the larger-scale flow setting is not altered. Climate change does not only lead to overall warmer temperatures, it may also change the large-scale dynamics, meaning that cyclones and cutoff lows may preferentially develop in different regions or with a modified frequency,

intensity or seasonality. In contrast, these experiments should be regarded as physically meaningful sensitivity experiments that allow studying the effects of changing one parameter (temperature or humidity) for a set of events. Specifically, one can investigate whether increased temperature and/or relative humidity lead to (i) higher precipitation totals, (ii) higher peak precipitation values, and/or (iii) changes in the precipitation pattern.

2.2.2 Results and discussion

In this section we discuss the results obtained with the COSMO-2 control simulations and sensitivity experiments for selected flood events during the last decades, and focusing on selected catchments (see Fig. 1.3). The analysis mainly focuses on the following questions:

- How well do control simulations with COSMO-2 represent the events?
- What is the typical response of the precipitation distribution with performing sensitivity experiments with increased specific humidity?

A more detailed analysis of how the different catchments respond in the different sensitivity experiments is presented later in chapter 4.2.

The quality of COSMO-2 control simulations

August 2005 event: As an example, we show the 2-day accumulated precipitation from a COSMO-2 control simulation for the August 2005 event and compare it with MeteoSwiss observations (gridded daily precipitation analysis RhiresD[1]), see Fig. 2.4. Both datasets clearly show the highest values of more than 200 mm along the main Alpine crest. Within Switzerland the general patterns agree very well; note that COSMO-2 has a higher horizontal resolution than the observations and therefore produces a more structured precipitation field.
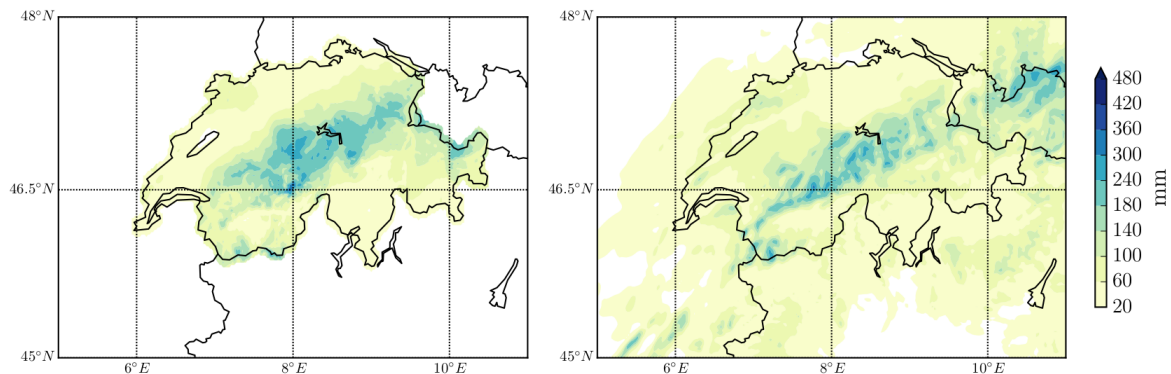

Figure 2.4: Observed (from RhiresD, left) and simulated (from COSMO-2, right) accumulated precipitation (in mm) during the two days from 00 UTC 21 to 00 UTC 23 August 2005.

---

[1] http://www.meteoswiss.admin.ch/content/dam/meteoswiss/de/service-und-publikationen/produkt/raeumliche-daten-niederschlag/doc/ProdDoc_RhiresD.pdf

Another, more hydrologically relevant test of the quality of the COSMO-2 simulation is to use the direct precipitation and temperature output from COSMO-2 as input to a QArea+ discharge simulation for the Schächen catchment. More details about the hydrological model QArea+ are given in chapter 3.3. The results of the Schächen discharge simulation and a comparison to observations are shown in Fig. 2.5.
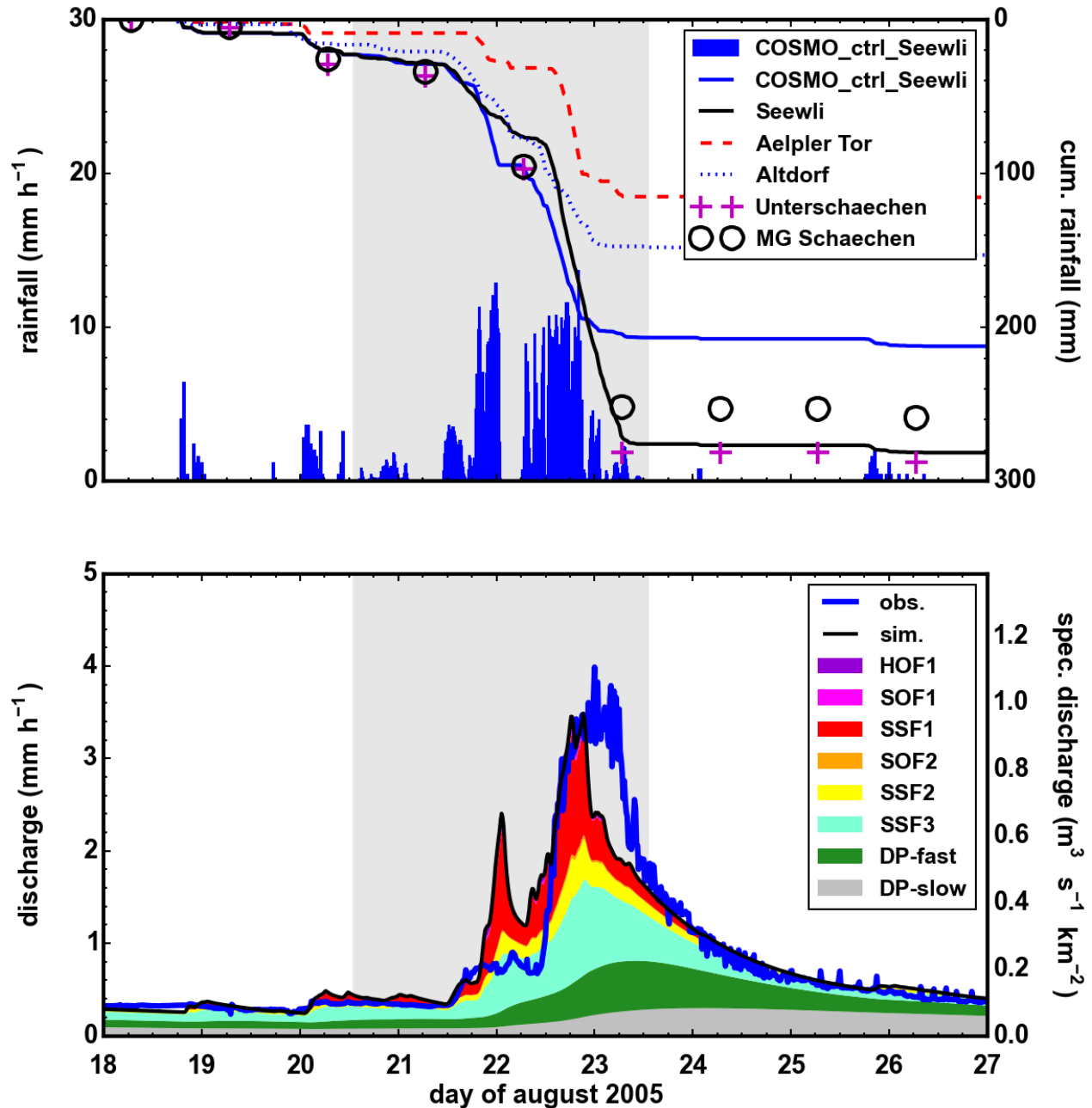

Figure 2.5: QArea+ simulations of the August 2005 event in the Schächen based on COSMO-2 control run rainfall for the 72-hour period indicated by the gray shading. Also shown is the cumulative rainfall at the stations Seewli, Aelpler Tor and Altdorf. The different colors indicate dominant runoff process (see chapter 3.2).

The upper panel shows that the accumulated precipitation from COSMO-2 reproduces the observed values at Seewli well until about 00 UTC 23 August (more than 200 mm) and produces too little rainfall on the following day. The discharge simulation using COSMO-2 precipitation at Seewli reproduces the observed evolution fairly well (see lower panel), in particular the steep increase after 12 UTC 22 August and the peak values exceeding 3.5 mm h^{-1}. This brief comparison of the COSMO-2 rainfall and observations illustrates the potential quality of convection-resolving simulations for heavy precipitation events that occurred in the last decade.

October 2011 event: In 2016, MeteoSwiss will further increase the horizontal resolution of its operational weather prediction model by replacing COSMO-2 with COSMO-1. After the October 2011 flood event, MeteoSwiss produced a pre-operational test simulation with COSMO-1 for this particular event. Figure 2.6 shows a comparison of the precipitation in the Bernese Oberland simulated with three different resolutions of the COSMO model. It becomes clearly apparent that whilst all model versions agree on the broad pattern of precipitation, the higher resolution versions produce a much more detailed precipitation distribution with generally larger variability and more pronounced peak values. The main reason for these important differences is the more accurate representation of topography when going to higher horizontal model resolutions. The significant difference between the two convection-resolving simulations COSMO-2 and COSMO-1 (middle and right panel) indicates the potential of further improving meteorological simulations of heavy precipitation events in Switzerland with the soon operational model COSMO-1.
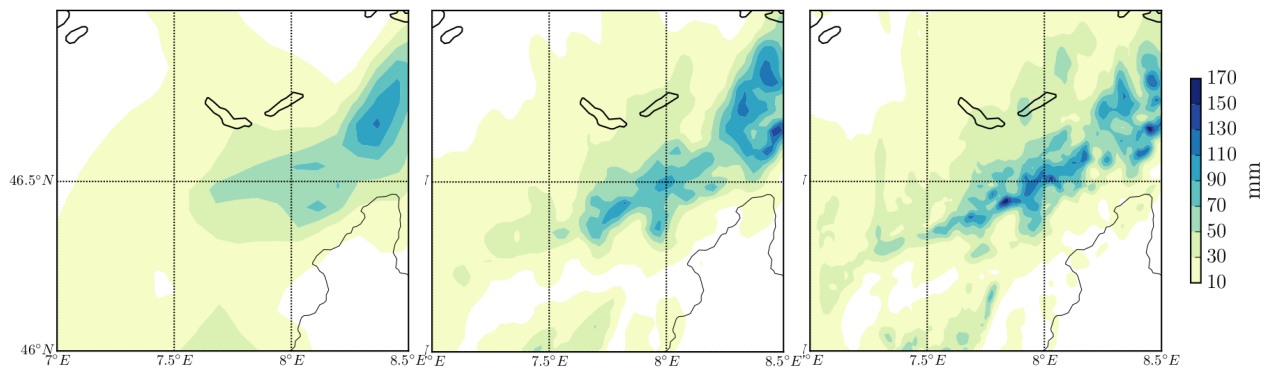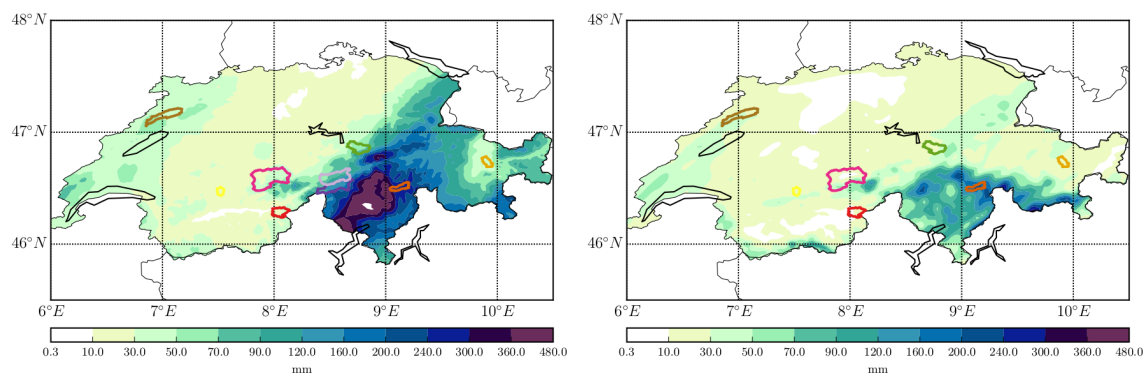

Figure 2.6: Accumulated precipitation from 12 UTC 09 to 12 UTC 10 October 2011 (in mm) from COSMO-7, COSMO-2 and COSMO-1 simulations, respectively (from left to right).

July 1987 event: Finally, we briefly show an example of a COSMO-2 control simulation for an earlier flood event in July 1987 (Fig. 2.7). In this case COSMO-2 strongly underestimates the 3-day accumulated precipitation. This event has therefore not been considered for the COSMO-2 sensitivity experiments, because the interpretation of the sensitivity experiments would be almost impossible if the control simulation is so far from representing the real event. The reason for this failure is most likely the fact that for this simulation initial and boundary data had to be taken from relatively coarse ERA-Interim reanalyses, whereas for later events higher-resolution and higher-quality initial and boundary fields were available from COSMO analyses at 7 km horizontal resolution. Note that in general the quality of

the initial and boundary fields is an essential prerequisite for successfully simulating heavy precipitation events with high-resolution regional models, and therefore it is more likely that COSMO-2 control simulations are successful (i.e., in agreement with observations) during the last about 15 years compared to earlier periods.

At this point it is appropriate to briefly describe why the quality of analysis fields and the capability to accurately simulate Alpine heavy precipitation events have increased since about the year 2000. A primary reason is the increased number of global observations, in particular from satellites and aircraft measurements, which provide a much better constraint on the actual state of the atmosphere also in oceanic (i.e., non-populated) regions. For instance from 1997 to 2002, the number of observations used for producing analysis data has increased by more than a factor of ten. Together with improved numerical models and data assimilation techniques, and with increased computational power, this allowed a substantial improvement of the quality of numerical weather prediction in general, and of heavy precipitation events in particular (Bauer et al. 2015).

Figure 2.7: Observed (from RhiresD, left) and simulated (from COSMO-2, right) accumulated precipitation (in mm) during the three days from 06 UTC 16 to 06 UTC 19 July 1987.

COSMO-2 sensitivity experiments: an illustrative example (August 2005 event)

First, the precipitation distribution in the CTRL and QV+30% simulations are compared for the August 2005 event. Figure 2.8a shows the two-day accumulated precipitation from 00 UTC 21 to 00 UTC 23 August in the CTRL simulation. High values exceeding 200 mm occur along the northern slope of the Alpine crest. This precipitation distribution is fairly realistic if compared to rain gauge observations (MeteoSwiss 2006). In the QV+30% experiment (Fig. 2.8b), precipitation increases compared to CTRL in the almost entire region north of the Alps (Fig. 2.8c). However, interestingly, the precipitation increase is particularly strong in the Jura and parts of the Swiss Plateau, i.e., in regions that do not experience very high values in CTRL. In contrast, in the mainly affected region of the central Alps, precipitation is only weakly increased in the experiment with increased humidity. This clearly shows that the precipitation response to increased humidity is strongly nonlinear, and that the most prominent increase does not necessarily occur in the areas mainly affected by the flood event.
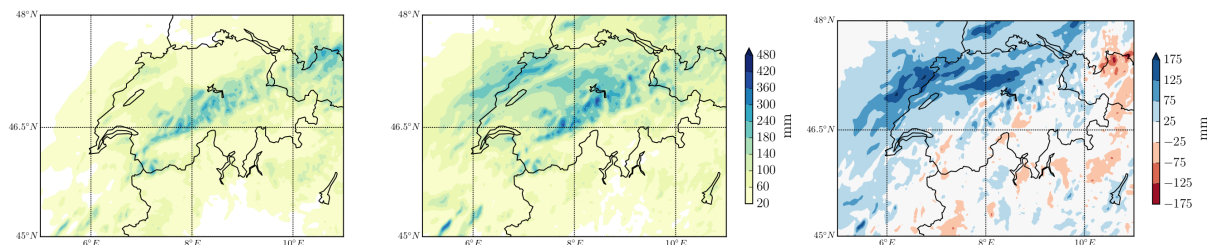
Figure 2.8: Two-day accumulated precipitation from 00 UTC 21 to 00 UTC 23 August 2005 (in mm) for (a) the CTRL and (b) the QV+30% simulations; (c) shows the difference between the two fields (QV+30% - CTRL).

A second example: the October 2000 event

Figure 2.9 shows the same difference field (QV+30% minus CTRL) for the October 2000 event. In this case there is a clear dipole in the difference field with a decrease in the Valais and a strong increase in the Ticino. Comparison with the CTRL experiment shows that this dipole leads to a fairly strong eastward shift of the overall rainfall pattern. This illustrates another important nonlinear effect that can occur in these sensitivity experiments: in some situations the modified latent heat release due to cloud formation can lead to changes in the local atmospheric flow and, as for this event, transport less moisture to the peak area of precipitation in the CTRL simulation (here the Valais) and more moisture to a less affected region in the CTRL simulation (here the Ticino). The main consequence of the increased humidity is then not a general increase but rather a shift of the resulting precipitation field.
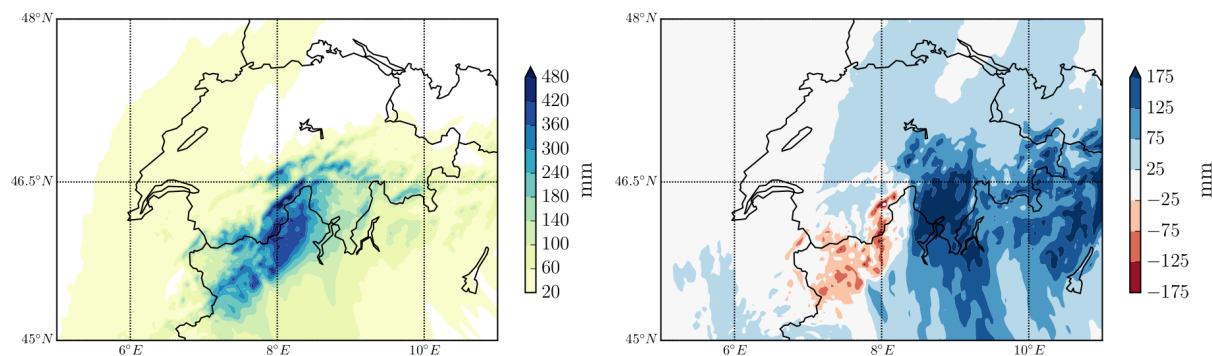

Figure 2.9: COSMO-2 simulation of the 3-day accumulated precipitation for the October 2000 event and the difference between from the COSMO-2 control and QV+30% simulations (right).

Summary and critical reflection

There are important findings from these experiments that are relevant when extrapolating to extremer events:

- The precipitation response to changes of the thermodynamic conditions (humidity and temperature) is highly complex in regions with varying topography. There is not a well-defined

precipitation response to, e.g., higher temperature or humidity that applies for all flow conditions and catchments.

- Large precipitation increases in the sensitivity experiments are limited to catchments that had only comparatively weak precipitation in the CTRL simulation.
- For some catchments and events, precipitation does not (strongly) increase when increasing humidity or temperature. This might be at first surprising, but it is related to the fact that with higher humidity and/or temperature, precipitation is likely triggered already "earlier" along the flow, i.e., at lower elevations, such that the flow reaching the higher elevation catchment might be even drier than in the control simulation.
- Very importantly: Changes in temperature and humidity lead to changes in cloud formation and latent heating in the atmosphere, which can change the local flow quite substantially. Therefore, even with the same large-scale flow conditions at the boundaries of the model domain, the small-scale flow changes near the Alps can lead to complex precipitation responses in small catchments. It is possible that the main precipitation area shifts by several 10 km, potentially leading to very large precipitation increase in some catchments.
- And finally, the resulting surface precipitation is not only a function of the available moisture, but also depends on the vertical temperature and humidity structure, and in turn on the detailed cloud microphysical processes from condensation to raindrop formation. These processes can vary strongly between events and regions and they also contribute to the nonlinear response observed in the sensitivity experiments.

3 Hydrology: What determines a catchment's flood behavior?

We here address how catchments' flood responses can be explained by landscape characteristics and meteorological boundary conditions. Then, we show how these insights help assess to what sort of characteristics of extreme rainfall catchments are most sensitive.

3.1 The importance of storage and drainage characteristics

Hillslopes can have widely varying runoff responses, but methods to explicitly describe these differences are not commonly used. This may be partly explained by knowledge gaps regarding these responses. Strongly reacting hillslopes are relatively well understood, but the responses of hillslopes with deeper subsurface drainage mechanisms are not.

Strongly reacting slopes are particularly relevant for runoff formation during events with high-intensity rainfall, because they have little storage capacity and runoff is quickly generated. Methods for mapping the occurrence of these kinds of slopes are well established for temperate and alpine regions (e.g., Scherrer and Naef, 2003; Markart et al., 2004). However, even in steep alpine regions these hillslopes rarely make up more than half of a meso-scale catchment ($40—400$ km^2). The remaining slopes have large storage capacities, and depending on the drainage time scale they may contribute considerably to a catchment's flood runoff formation during long-duration events. To better understand the storage and drainage processes of alpine slopes, the NFP61 project SACflood was instigated. New tools for mapping and modeling the dominant runoff processes (DRP) were developed to determine their influence on catchment-scale flood behavior. Some key observations are highlighted here to demonstrate why studies of extreme floods require these tools. More detailed information can be found in Smoorenburg (2015). These tools were used in this project to evaluate the sensitivity of flood runoff to changes in precipitation input.

Detailed field observations at various slopes in the Schächen catchment revealed that even steep alpine slopes can store so much water during event time scales that they contribute negligibly to flood formation at the catchment scale. This was observed for slopes with thick (>10 m) deposits of Quaternary sediments (typically moraines and rockfall debris). On the other hand, a creeping landmass slope started to contribute to flood runoff during several large rainfall events of longer duration.

These behaviors are illustrated with the runoff produced at some exemplary sites during the 2-year event of October 2012. In both the Schlücht creeping landmass slope and the Gadenstetten debris deposit, all rainfall percolates to a deep groundwater body, from where it drains via a spring at the bottom of the slope (Figs. 3.1 and 3.2). This process also dominated during a sprinkling experiment in Schlücht, whereby more than 700 mm was applied at rates of 12 mm h^{-1}. The groundwater table in the fractured rock of the creeping landmass slope at ~5 m depth rises by more than 2 m during an event. The outflow of the spring corresponds with the groundwater table variations. The outflow can be considerable during extreme events, but the rising limb and flow peak lag many hours behind the rainfall inputs and the runoff response of the Schächen catchment itself (Fig. 3.3). The response of the

Gadenstetten slope is even more delayed, such that it contributes little to the flood runoff formation in the Schächen.

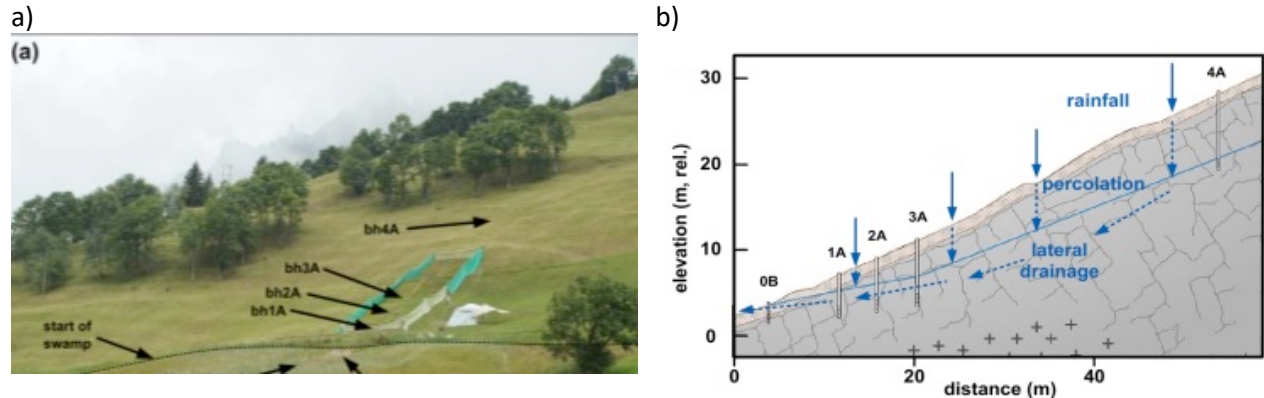a)   b)

Figure 3.1: Schlücht creeping landmass slope (a), and the relevant processes (b). About 1 m of permeable soil is covered by grassland and underlain by heavily fractured flysch bedrock until at least 9 m depth. No runoff formation occurs on or in the soil. Instead, the water percolates to recharge the groundwater body in the fractured rock, from where it resurfaces at a line of springs downslope. The numbers indicate the piezometers; spring discharge was measured with a V-notch weir.

a)   b)
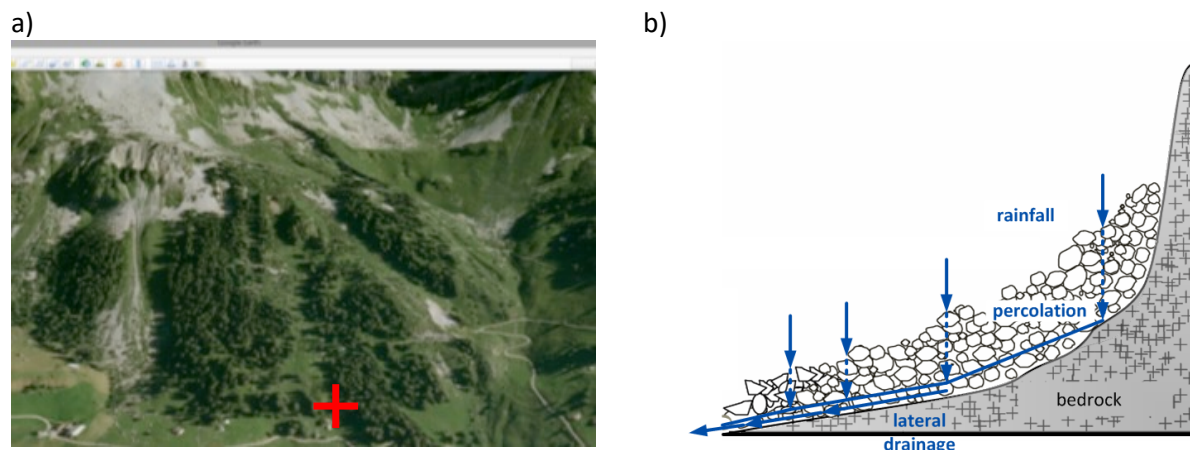
Figure 3.2: Gadenstetten rockfall / moraine deposit (a; courtesy Google Earth), and the relevant processes (b). A shallow but permeable soil supports grassland and forest, formed on a coarse debris deposit of tens of meters deep. Spring outflow was measured with a V-notch weir (red symbol).

Slopes like Schlücht become important during long duration rainfall events. Determining how much of the catchment reacts like Schlücht or Gadenstetten is required for an adequate description of its runoff behavior. For example, the Wissenboden headwater, a subcatchment of the Schächen, has a small fraction of well-connected fast reacting areas, but is otherwise dominated by thick deposits similar to the Gadenstetten slope. The fast reacting areas produce the rapid runoff fluctuations, whereas the rest of the catchment holds most rainfall (about 120 of the 150 mm of the event rainfall). The hydrograph (Fig. 3.3) looks flashy, but the overall response magnitude is only slightly larger than in the Schächen, although the rainfall input was much larger (Smoorenburg, 2015).
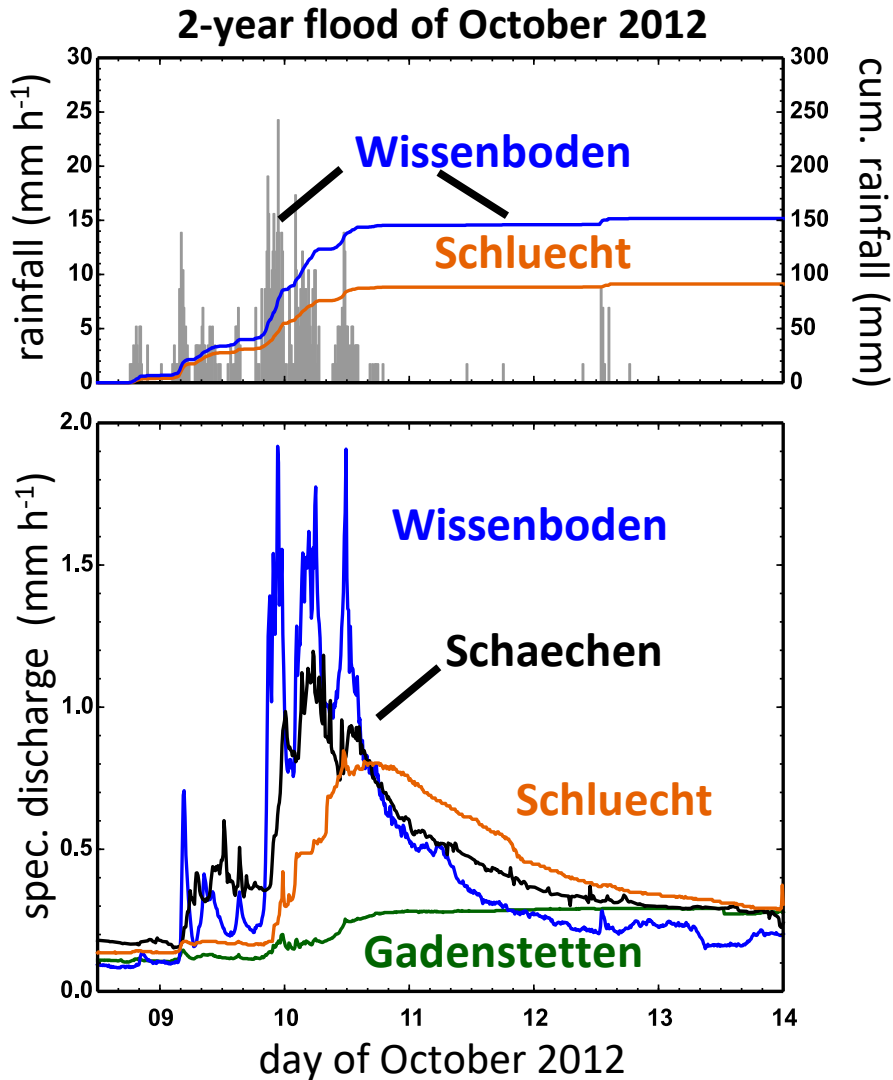
Figure 3.3: Rainfall and discharge at three test sites in the Schächen during the October 2012 event. Top: The rainfall at the Schlücht and Gadenstetten slopes was similar to the average rainfall of the Schächen catchment, at Wissenboden it was 50% larger. Bottom: hydrograph of the Schächen and at the three sites. The Schlücht slope contributes significantly, but with some delay, whereas the Gadenstetten response is not relevant for flood generation. The flashy response of Wissenboden is caused by a strongly reacting small tributary, the thick deposits dominating the rest of the catchment only contribute negligibly to flood runoff.

3.2   The DRP mapping and modeling framework

A new mapping technique for characterizing the dominant runoff processes in alpine areas was developed to estimate the drainage time scales of slopes with large storage capacity (Smoorenburg, 2015). The technique characterizes deep subsurface drainage processes to assess contributions of slopes during long-duration rainfall events. The mapping technique complements the methods for classifying

dominant runoff processes (DRP) occurring in the shallow subsurface (<1 m) since the early 1990s (e.g., Scherrer and Naef, 2003; Schmocker-Fackel et al., 2007). These techniques characterize the response of areas that react strongly to intense precipitation and require high-resolution soil information. In contrast, the scheme of Smoorenburg (2015) classifies processes at the hillslope / landform scale, on the basis of interpretations of orthophotos, geo(morpho)logical maps, and high resolution digital terrain models, which are available for the contiguous Swiss Alps. The classification of the different landform / sediment type configurations are summarized in Fig. 3.4. The classification scheme itself is presented in Fig. 3.5. Slopes with 'Deep Percolation' (DP) runoff process are expected to have a more damped reaction than slopes with 'Subsurface Stormflow' (SSF). The Gadenstetten slope is an example of the extremely damped DP-debris2 type, whereas the Schlücht slope is typical for the more responsive DP-rock class.

By applying this scheme to catchments, Dominant Runoff Process (DRP) maps can be produced. Figure 3.6 shows DRP maps of three strongly contrasting catchments. The classes consist of similarly reacting runoff formation mechanisms; the numbers indicate the process intensity. Higher numbers denote more damped responses (i.e., more storage). The classification yields one Hortonian Overland Flow class (HOF1), two Saturation Overland Flow classes (SOF1 and SOF2), three Subsurface Stormflow classes (SFF1, SSF2, SSF3), and three Deep Percolation classes (DP-rock1, DP-debris1, and DP-debris2). The DP classes, where drainage occurs at large depth in either fractured rock or in thick sediment deposits, have the most strongly damped responses. HOF1, occurring on impermeable surfaces like rock walls, is the fastest reacting class.

For ease of interpretation, the classes are clustered into the following four groups, according to their reaction to precipitation:

o **Strong:** fast or very fast reacting areas with little to medium storage capacity, contributing already during small events.
o **Damped:** areas with large storage capacity with delayed drainage, starting to contribute only during events of long duration.
o **Little contributing:** areas with large storage capacities with virtually no drainage response within event time scales, contributing only marginally, even during the largest floods.
o **Very fast, but unconnected:** areas with little storage capacity and fast response (HOF1, SOF1 and SSF1), whose generated runoff does not discharge directly in a river but re-infiltrates into below lying DP-type landforms.
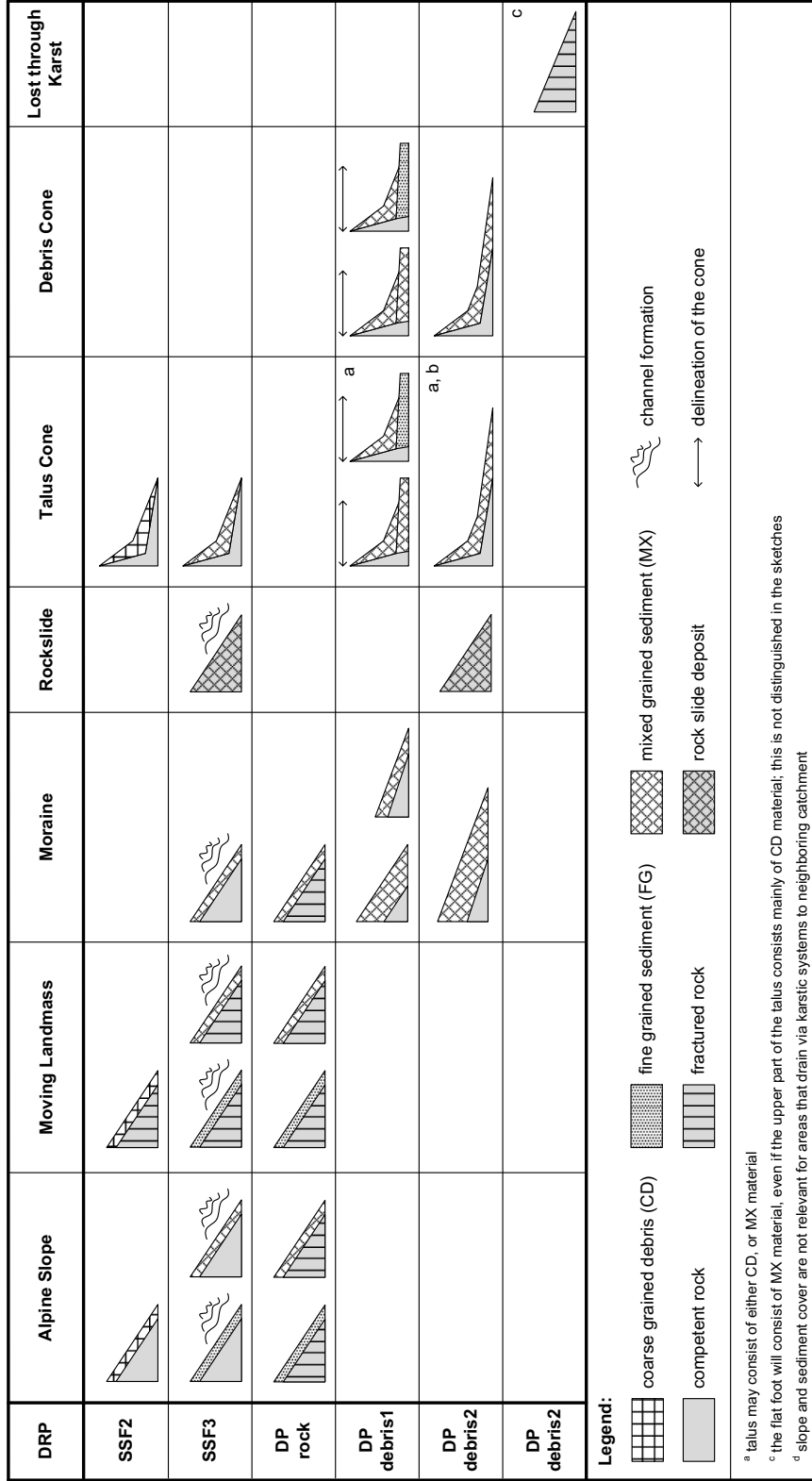
DRP	Alpine Slope	Moving Landmass	Moraine	Rockslide	Talus Cone	Debris Cone	Lost through Karst
SSF2							
SSF3							
DP rock							
DP debris1					a		
DP debris2					a, b		
DP debris2							c

Legend:

- coarse grained debris (CD)
- competent rock
- fine grained sediment (FG)
- fractured rock
- mixed grained sediment (MX)
- rock slide deposit
- channel formation
- delineation of the cone

a talus may consist of either CD, or MX material

c the flat foot will consist of MX material, even if the upper part of the talus consists mainly of CD material; this is not distinguished in the sketches

d slope and sediment cover are not relevant for areas that drain via karstic systems to neighboring catchment

Figure 3.4: Landform configurations, found in mountainous hillslopes with large storage potential, defining dominant runoff process classes. The diagrams illustrate differences and similarities in shape, sediment texture and bedrock permeability (not drawn to scale; adapted from Smoorenburg, 2015).
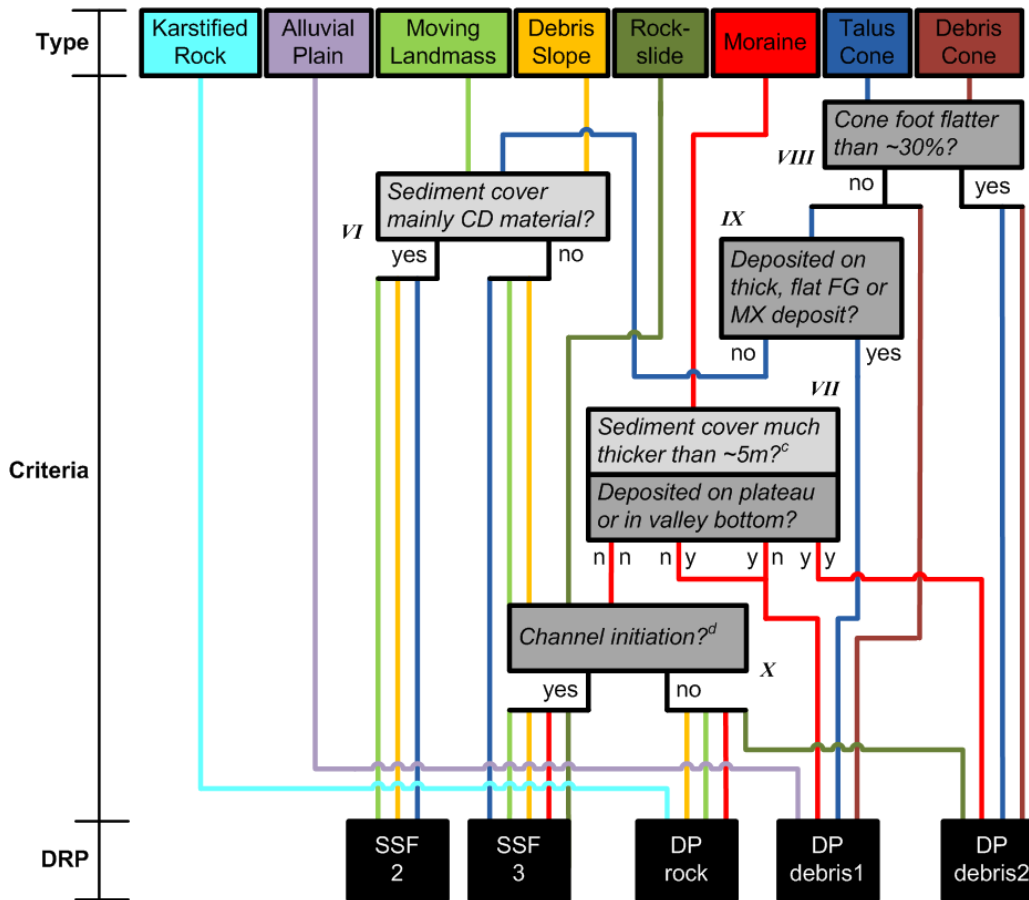
Figure 3.5: Decision scheme to classify dominant runoff processes (DRP) in landforms with large storage capacity. The processes in the different landforms (colored boxes at the top) are classified according to the connected criteria (grey boxes), resulting in the DRP classes at the bottom (different types and intensities of subsurface stormflow, SSF, and deep percolation, DP; adapted from Smoorenburg, 2015).

The four groups 'strong', 'damped', 'little contributing', and 'very fast but unconnected' allow assessing how a catchment's landscape characteristics influence the flood response. The Hinterrhein catchment has the largest fraction of 'strongly' reacting areas, and few areas that 'contribute little' (Fig. 3.7). This explains the strong runoff response. The Schächen and Dischma catchments have similar fractions of 'strongly' reacting areas, as well as 'little contributing' areas, but the Schächen has more areas with 'damped' response. These areas could have contributed to the markedly stronger response of the Schächen during the four largest events (Fig. 1.2).
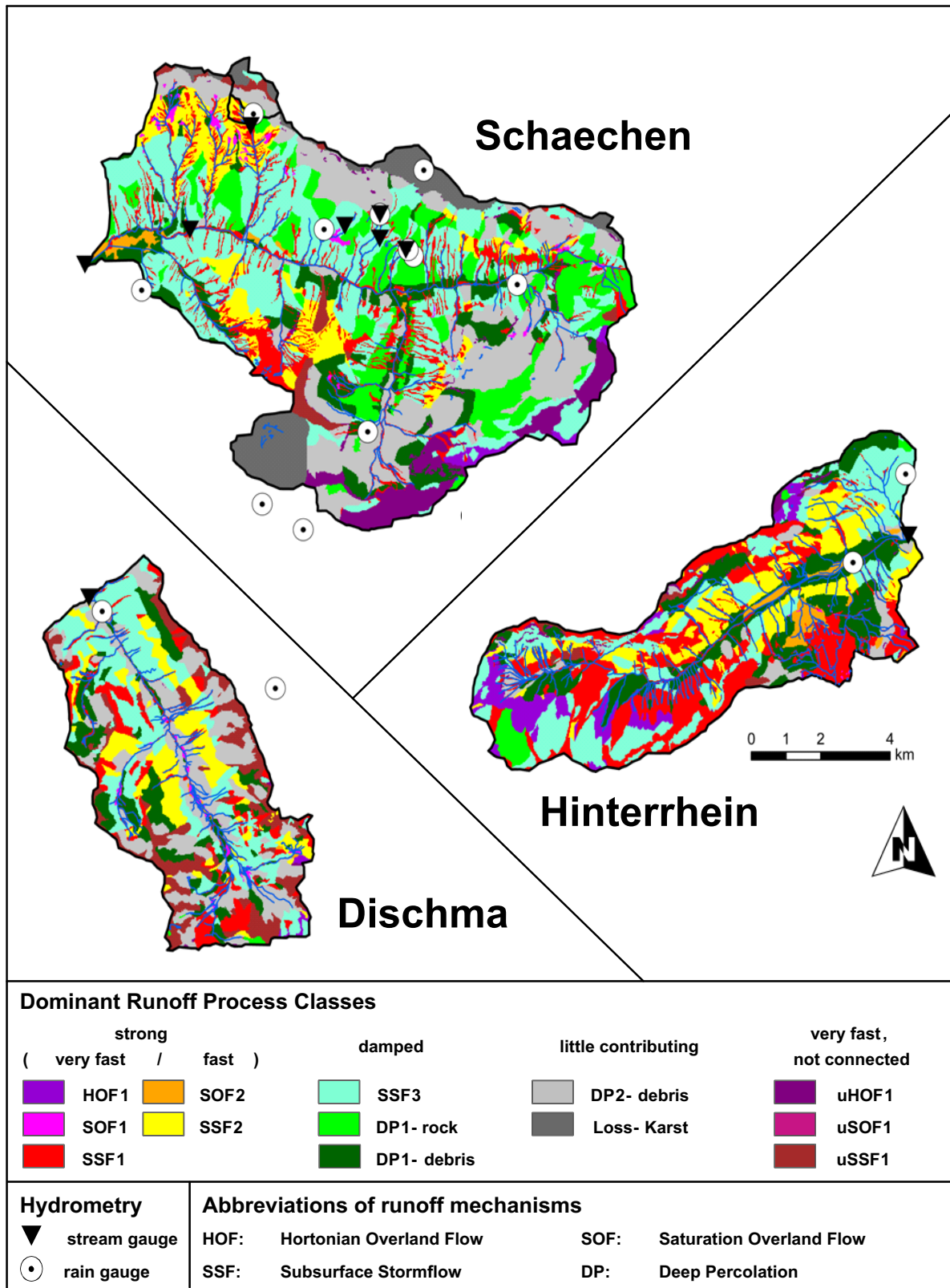
Figure 3.6: Dominant runoff process (DRP) maps obtained from applying the decision schemes of Smoorenburg (2015) to the Schächen, Hinterrhein, and Dischma catchments (displayed at equal scales).

The Dischma catchment has more 'unconnected' areas than the Hinterrhein and Schächen. The catchment would have twice as many very fact reacting areas if connectivity was not accounted for. In the classification scheme, only areas are mapped that are never directly connected, although there may be areas that only connect during certain events (e.g., high intensity thunderstorms). Subsurface connectivity may be critical too. In the Dischma catchment many SSF2 and SSF3 areas are connected to the main stream via thick sediment deposits, whereas in the Schächen catchment, they are often directly connected to a stream. Therefore, the mapping procedure does not fully reflect the differences between the Dischma and Schächen catchments (Smoorenburg, 2015).

The DRP maps reflect well the observed behaviours of the three catchments. They can explain, why the runoff response of the Hinterrhein is more sensitive to rainfall intensity than the Dischma and Schächen catchments and why these are more sensitive to the event volume and duration. The DRP map of the Schächen also correctly describes differences in runoff response observed at various subcatchments of the Schächen.
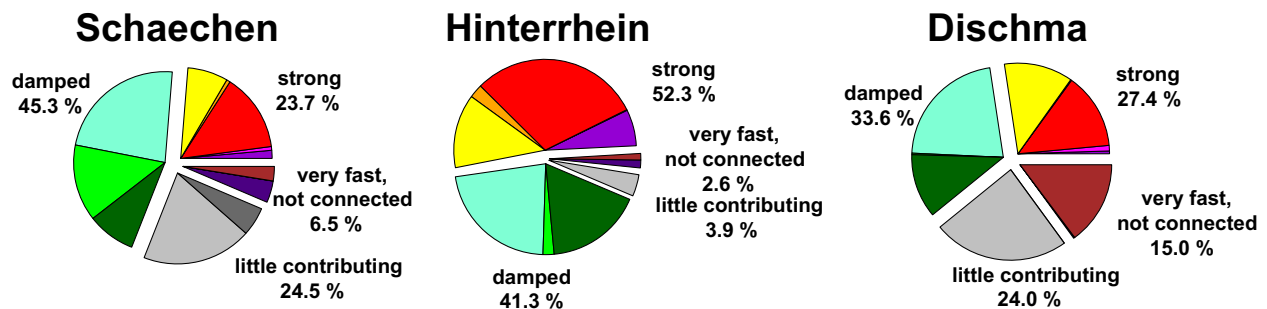
Figure 3.7: Distributions of dominant runoff processes (DRP) in the Schächen, Hinterrhein and Dischma catchments. The DRP classes are clustered into four groups ('fast', 'damped', 'little contributing', and 'very fast, not connected').

3.3 Rainfall-runoff modeling with the DRP maps using QAREA+

Smoorenburg (2015) also enhanced the spatially distributed rainfall-runoff model QAREA to QAREA+ by including the delayed DRP types. Each of the mapped DRP types are simulated by a dedicated combination of linear and nonlinear reservoirs for representing the dominating runoff mechanism (Fig. 3.8). The structures for the different processes are similar to the ESMA-type model structures used in models like HBV, PREVAH, and LARSIM.
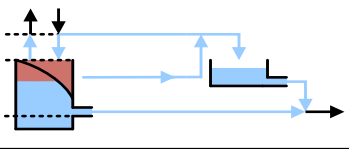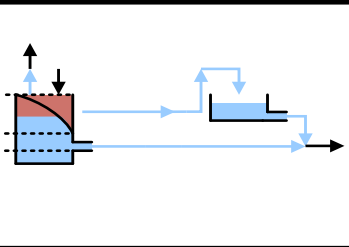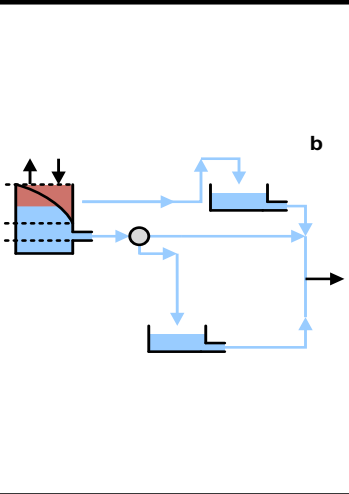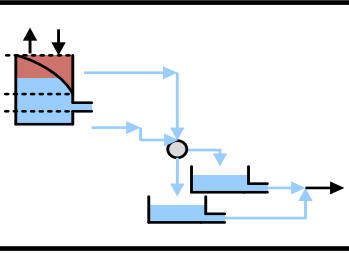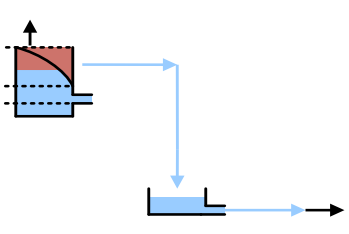
The model simulates each DRP separately. The parameters for all the processes were estimated on the basis of small-scale observations like sprinkling experiments as presented in Scherrer (1996) and Scherrer et al. (2007) and on observed flood responses in small subcatchments (<2 km^2) in the Schächen. The model parameterization reflects the mapped landform properties and was kept parsimonious by sharing parameters between the classes as much as possible (Smoorenburg, 2015).

With this parameterization the model could adequately predict small and large floods in the three contrasting catchments without catchment-specific parameter adjustments. As examples, simulations of

the largest flood on record in the Schächen catchment, and the second-largest floods on record in the Hinterrhein and Dischma catchments are resented (Fig. 3.9). For these events, the flood-producing precipitation inputs are well understood; the snow lines were high, there was little snowmelt, and the temporal development of the catchment-averaged precipitation could be adequately estimated (Smoorenburg, 2015).

The floods peaks in the strongly reacting Hinterrhein catchment are among the highest in the Swiss Alps. They were caused by 6 to 12 hour long periods with rainfall intensities well over 10 mm h^{-1} with some intensity spikes exceeding 20 mm h^{-1}. In the Schächen catchment, intensities and peak discharges of the most extreme floods are lower. In the Dischma catchment, they are even smaller. Its largest flood belongs to the smallest in alpine catchments of similar size in the Swiss Alps

The good agreement between simulated and observed discharges without catchment-specific parameter adjustments suggests that the developed mapping and modeling tools describe the runoff formation processes adequately in the different catchments.

sediment cover thickness	runoff response strength	DRP	Model Structure
shallow (s; <~0.5m) or medium (m; ~0.5 to ~1.0m)	strong	[a]HOF1	
		[a]SOF1	
		SOF2	
		[a]SSF1	
		SSF2	
thick (t; ~1 to ~5m) or very thick (vt; >~5m)		SSF2	
	damped	SSF3	
		DP rock	
		DP debris1	
	little contribu-ting	DP debris2	
		DP debris2	

[a] very fast reacting DRP that can be mapped as being 'unconnected,' i.e., all generated runoff re-infiltrates into a DP-type landform

[b] the SSF1 model is parameterized according to the other SSF classes, but has no slow groundwater component

Figure 3.8: The first column indicates the sediment cover thickness of the different DRP, the second their reaction group. Column 4 shows the QAREA+ model structures, developed for the different DRP (column 3).
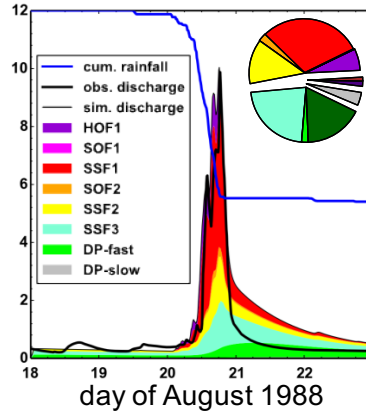
Schaechen

Δq : 3.3 mm h⁻¹

P : 11 mm h⁻¹ (132 mm / 12 h)
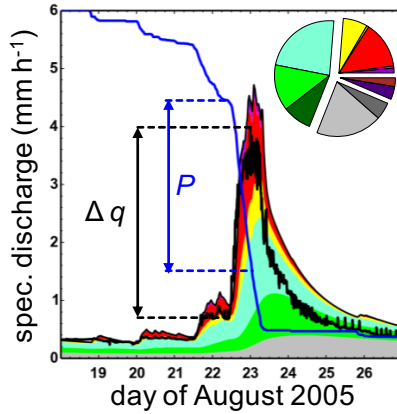
Hinterrhein

Δq : 9.5 mm h⁻¹

P : 15 mm h⁻¹ (128 mm / 8.5 h)

Dischma

Δq: 1.2 mm h⁻¹
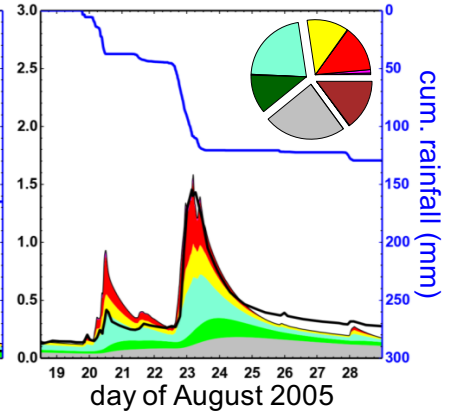
P: 4.6 mm h⁻¹ (60 mm / 13 h)

Figure 3.9: QA$_{AREA}$*⁺ simulations of the largest flood on record of the Schächen, and the second-largest floods on record of the Hinterrhein and Dischma (note the different scales for specific discharges). The flood-producing parts of the rainfall event are indicated above the graphs, according the definitions displayed in the Schächen graph, together with the increase in specific discharge rates. The colored fillings of the hydrographs indicate the contributions of the areas of each DRP, the proportions of each DRP are presented in the pie chart insets (after Smoorenburg, 2015).*

4 Extrapolation to extremer events

4.1 Extrapolations based on synthetic rainfall

4.1.1 Precipitation events from other catchments

The DRP mapping/modeling tools were used to assess how differences in the distribution of dominant runoff processes influence catchment responses and flood behavior and how far differences in meteorological forcing are responsible. This is illustrated by exchanging the rainfalls of the most extreme events between the studied catchments (Fig. 4.1).

The rainfall that produced the largest flood on record in the Schächen had the largest rainfall sum of the three extreme events of Fig. 3.9. In the Hinterrhein, such a rain would produce a much larger peak than in the Schächen, but in the Hinterrhein, it would count only as a 10-year flood. This is mainly because the rainfall intensities were much smaller than those that produced the largest floods in the Hinterrhein.

The average intensity of the Hinterrhein 1988 was roughly 40 to 60% higher than 2005 in the Schächen, a rate that seems unlikely to occur during so many hours in this part of the Alps. Such an event would produce a 20% higher flood in the Schächen than in August 2005.

The Dischma floods produced by such events would be comparable to those of the Schächen. However, as mentioned in chapter 3.3, the Dischma may react less than the DRP map indicates, as many slopes with damped runoff responses are not directly connected to the main stream network.
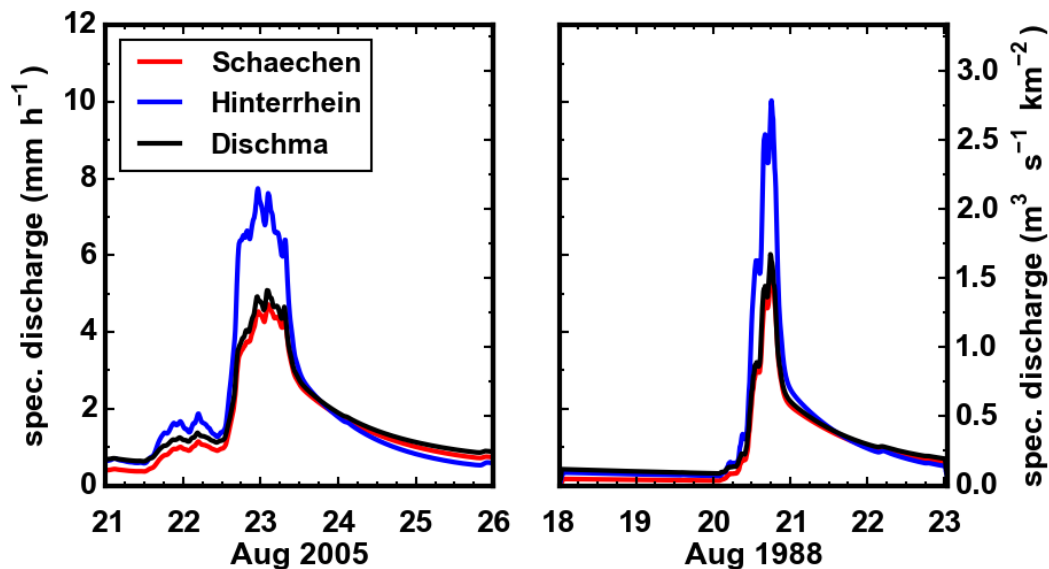

Figure 4.1: Discharge simulations when applying the rainfall observed in August 2005 in the Schächen catchment to the Hinterrhein and Dischma catchments (left), and applying the rainfall of August 1988 in the Hinterrhein to the Schächen and Dischma catchments (right).

4.1.2 Applying constant rainfall intensities for long durations

By applying constant rainfall intensities of equal durations, the reactions of catchments with different DRP areas can be directly compared. The simulations presented start with wet antecedent conditions. The model's unsaturated zone storages of all DRP were set to field capacity and the slow groundwater storages filled to equal levels, such that their combined outflows produced 0.5 mm h^{-1} discharge. The new rain was added after a dry period of 24 hours.

The responses of the Schächen and Hinterrhein to a 24-hour, 10 mm h^{-1} rainfall event are presented in Figs. 4.2 and 4.3. As the bottom panels of the graphs shows, the different DRP have the same reaction in all catchments. The individual reactions of catchments are caused by the different areas occupied by each DRP, as defined by the DRP maps. The 'fast' DRP reaches a steady state within 24 hours with runoff fluxes close to the rainfall rates. Areas with 'damped' responses are then not yet fully contributing; 'little-contributing' areas produce runoff rates below 25% of the rainfall intensity and increase only slowly.
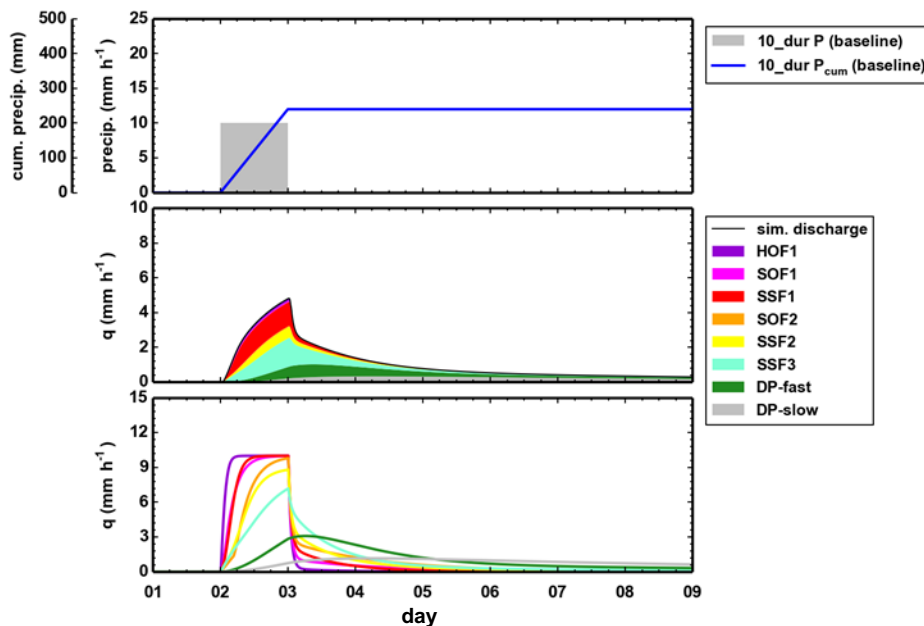

Figure 4.2: Response of the Schächen to a 24-hour rainfall of 10 mm h^{-1}. The top panel presents the rainfall and cumulative rainfall, the middle panel the runoff response with the contributions from the different DRP areas. The bottom panel specifies the runoff response of each DRP per unit area.
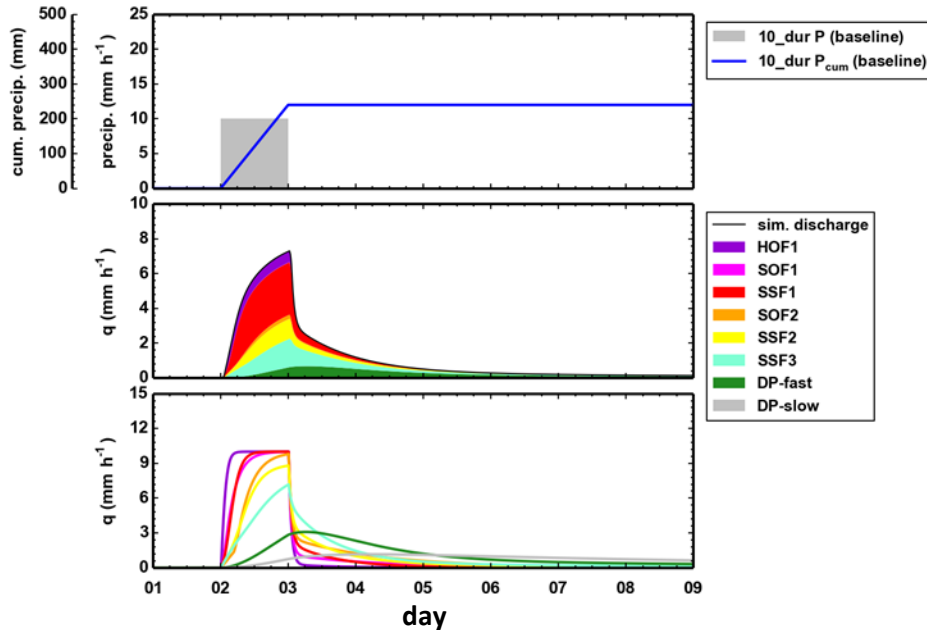
Figure 4.3: Response of the Hinterrhein to a 24-hour rainfall of 10 mm h^{-1}. Panels as in Fig. 4.2.

In Fig. 4.4, sensitivity experiments are repeated for different intensities and higher time resolution. Shown are the peak discharges. Again, the Dischma and Schächen react similarly, although DRP maps differ. This suggests that rain characteristics are the main reason for the difference; it simply rains about twice as much in the Schächen as in the Dischma. The runoff coefficient in the Hinterrhein reaches 80%. In the Dischma and Schächen, the relatively modest increase in peak discharge is due to the damped response of the DP-type areas, which make up a third to half of the catchment.
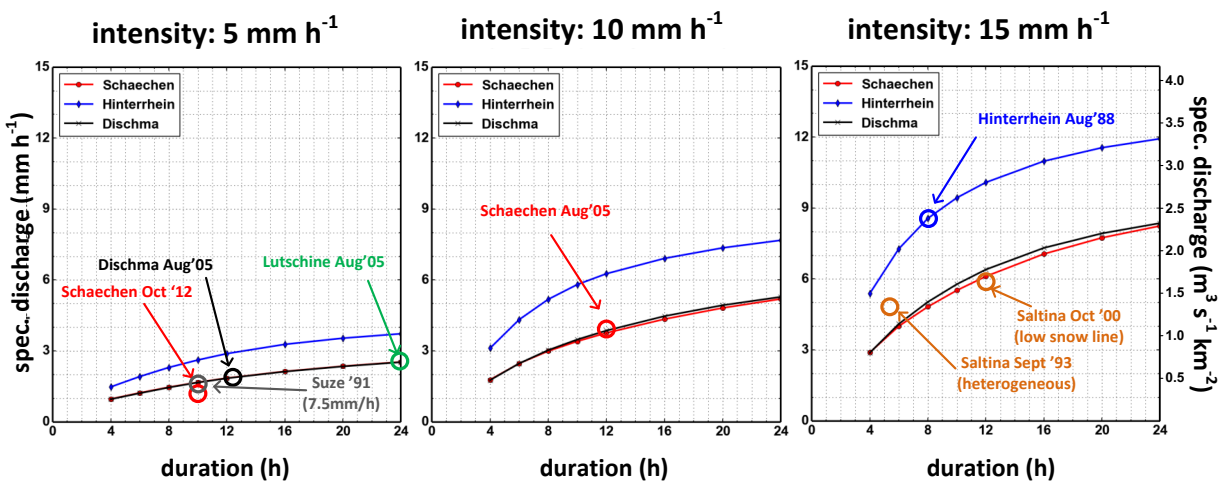

Figure 4.4: Peak flows of the Schächen, Hinterrhein and Dischma when subjected to constant rainfall with different intensities and an antecedent flow of 0.5 mm h^{-1}. Indicated are also the largest observed flood peaks of the Schächen, Dischma and Hinterrhein and a small flood in the Schächen in 2012, together with the measured rainfall intensities. The largest floods of the Lütschine in Gsteig, Saltina in Brig and Suze in Biel are also indicated.

36

Comparison of the simulations with observed events in different catchments

Figure 4.4 shows the peak flows resulting from rains with increasing intensities and duration, as derived from Qarea+ simulations. Data from the largest observed events from these catchments are included, as well as from the Lütschine (Gsteig), Saltina (Brig) and Suze (Biel). For these catchments, detailed hydrological studies are available, including DRP maps. The displayed mean rainfall intensities and duration have been derived from the main phase of these events.

The Lütschine (Gsteig) and the Weisse Lütschine (Zweilütschinen)

The Lütschine produced five exceptional floods since 2000. Outstanding among them was the 2005 event. The Lütschine drains a complex catchment with large glaciers and elevation ranges and extended areas with delayed runoff response. Areal rainfall is difficult to assess due to the rugged topography and missing data from the higher regions. As Fig. 4.4 shows, the Lütschine belongs to the family of delayed reacting catchments. This is in agreement with the existing DRP map and simulations with the Qarea model (Naef & Lehmann, 2012).

Saltina (Brig)

The Saltina was also hit by two exceptional floods, one in September 1993, the other in October 2000. Both events with exceptional rainfall amounts lasted for several days. The Saltina is also delayed reacting (Fig. 4.4). This was already shown by VAW (1994b), based on early versions of DRP mapping and model simulations.

Suze (Biel)

The largest flood in the Suze (Biel) occurred in December 1991, when the channel capacity was nearly exceeded. A moderately higher flood would have produced severe damage in Biel. Thanks to COSMO-2 simulations made in this project, the sensitivity of the rainfall field to changes in boundary conditions is known. However, as runoff production in the Suze catchment is dominated by large karstic systems, extrapolation to higher floods would require a specialized field study (VAW, 1994a; Hybest et al., 2013).

The Suze, too, belongs to the slowly reacting catchments, as well as the Lütschine, Schächen and Saltina. All of them experienced, or narrowly escaped, disastrous floods in the last decades, although they produced, in comparison to the Hinterrhein, only moderate flood peaks. This illustrates the importance of considering landforms with large storage potential and their drainage behavior in alpine environments when extrapolating to extreme floods.

The extreme floods indicated in Fig. 4.4 show that many catchments lie rather along the Dischma/Schächen line, indicating that large storages are available to damp the flood runoff response. This was also concluded in the detailed studies made for these catchments.

Comparison of these events and simulated responses clearly shows that a classification of the catchment flood response depends on the flood-producing-rainfall characteristics; a rainfall of 5 mm h^{-1} could only cause flood peaks comparable to the largest floods caused by higher intensities when it rains

for much more than 24 hours. On the other hand, differences between the catchments cannot be explained by differences in rainfall intensities alone, as was also concluded from the transfer of rainfall inputs in the previous section.

4.1.3 Maximum rainfall intensity occurring at the end of the event

Delayed reacting areas increase their contribution during a prolonged event. Therefore, high intensity rain spells, falling at the end of an event, have a larger impact on flood peaks than at the beginning. Usually, rainfall intensities decrease towards the end of an event – but not so during the 1987 Reuss flood: The catastrophic flood peak was caused by a rain spell in the last hour of the event with an intensity of 40 mm h^{-1}. Had this spell occurred at the beginning or in the middle of the event, peak discharge and damage would have been much smaller.

Because the available data do not allow a reliable simulation of the 1987 flood, the impact of this effect is demonstrated with the Schächen 2005 event. To this purpose, the August 2005 rainfall evolution is 'mirrored', which leads to the highest intensities occurring toward the end (Fig. 4.5). This 'mirrored event', with the same duration and average intensity, increases the flood peak by 20%. This effect can therefore be pronounced in delayed reacting catchments; however, its low probability also reduces the probability of the resulting floods.
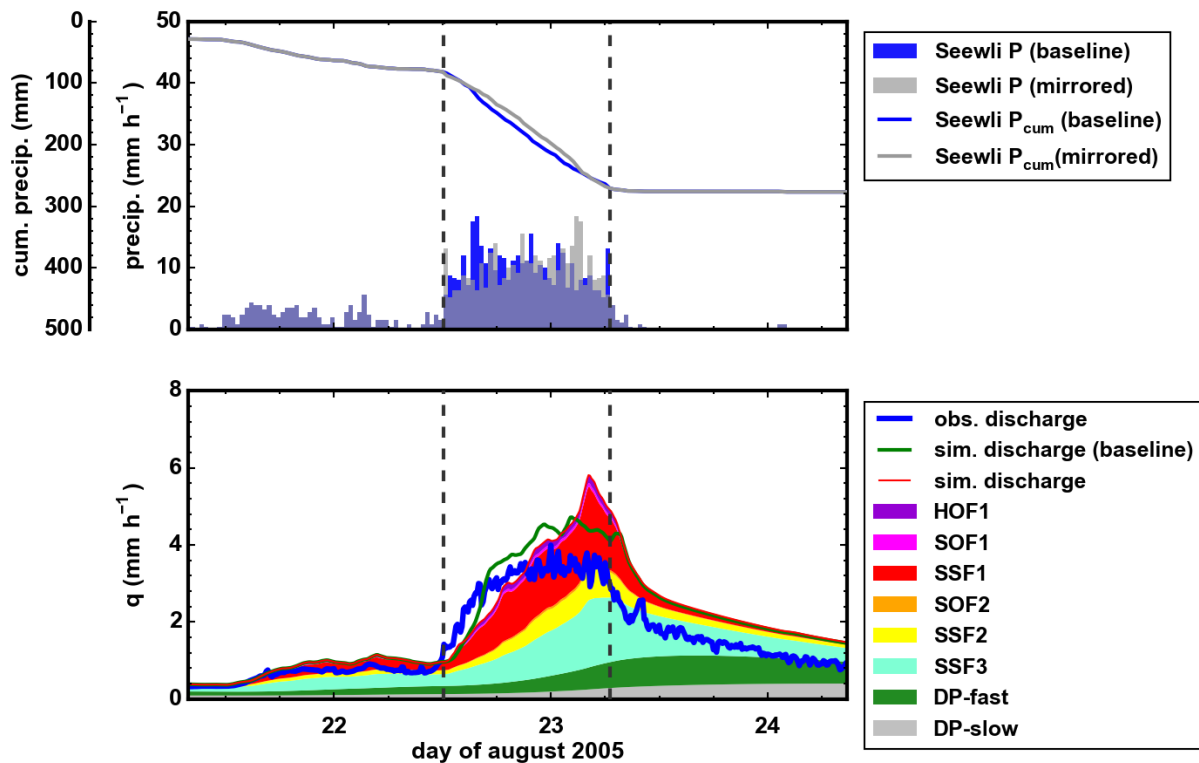

Figure 4.5: The Schächen 2005 event with the rainfall period between the vertical dashed lines mirrored, such that the highest intensities occur at the end the period, yielding a roughly 20% higher discharge peak.

4.1.4   Modifying rainfall of past extreme events

In these simulations, the rainfall amounts of the largest observed events in the three catchments was modified between the start of the rising limb of the flood hydrograph and the moment of peak flow between -30% to +50% in steps of 10% (Fig. 4.6). In this way, the duration and intensity sequences of natural events were preserved, unlike the block rain simulations shown in Fig. 4.4.

Rainfall amounts are comparable in the Schächen and Hinterrhein and much smaller in the Dischma. Increases of the peaks in the Dischma and the Hinterrhein are nearly linear, however, the Hinterrhein is much more responsive. The Schächen reaction is far below the Hinterrhein. But due to the special combination of duration and intensity sequence, the slope of the curve increases with increasing rainfall amounts; therefore the Schächen is not reacting proportionally. A model should be able to simulate this effect correctly in the extrapolation range.

4.1.5   What did we learn?

The results of these various types of numerical experiments give insight into the different reactions of rivers to increasing precipitation and illustrate the complex interaction of precipitation and storage/drainage characteristics in the formation of extreme floods in catchments with different distributions of Dominant Runoff Processes. To this purpose, synthetically increased rainfalls with no physical background were employed. The question remains how to define physically plausible rainfall events producing floods with high return periods. Extrapolations based on COSMO-2 experiments have a solid physical basis; in the following chapter, they are combined with hydrological simulations to produce a set of plausible events.
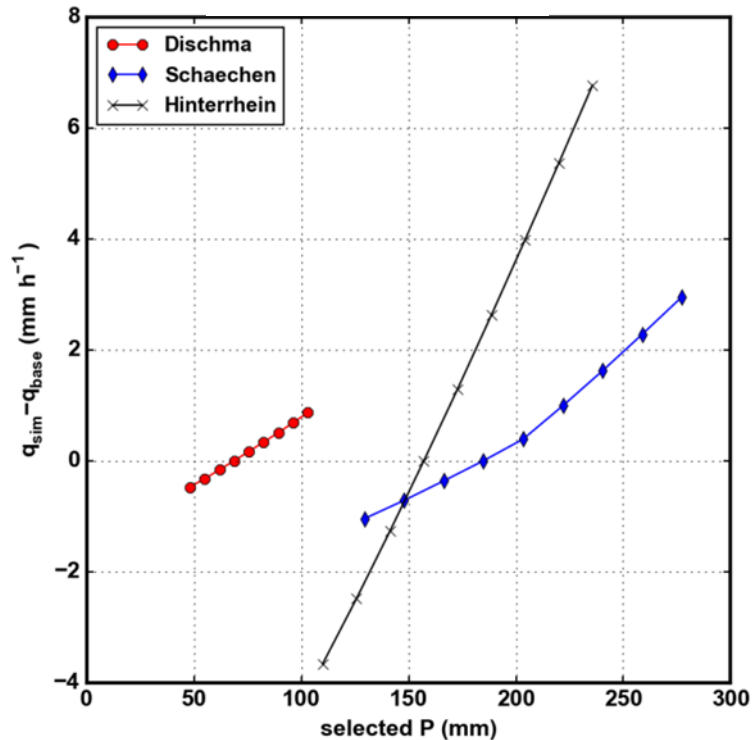
Figure 4.6: Changes in peak discharge in the three catchments due to modifications of the rainfall that produced the large events presented in Fig. 3.9 (the base line simulations); rainfall between the start of the rising limb of the hydrograph and the moment of observed peak flow is changed from -30% to +50% in increments of 10%.

4.2 Extrapolations based on COSMO-2 simulations

4.2.1 Approach

The COSMO-2 simulations of the largest flood producing events (see Section 2.2.2) were used as input fields to the QArea+ model. The events considered in detail were December 1991 (Suze), September 1993 (Saltina), October 2000 (Saltina, Lütschine), August 2005 (Schächen, Lütschine, Dischma), August 2007 (Lütschine, Suze) and October 2011 (Lütschine). COSMO-2 simulations of events before 1991 showed larger discrepancies between model results and rainfall measurements, especially in alpine regions (see discussion in Section 2.2.2). Therefore, simulations of the catastrophic flood in the Reuss in 1987 and the large events in the Hinterrhein 1987 and 1988 did not provide usable results.

In Figs. 4.7 and 4.8, COSMO-2 results for the events mentioned above are presented. The first bars show the reconstructed rainfall amounts in the six catchments. The hatched parts indicate rain; the rest fell as snow. The blue bars show resulting rainfalls when the specific humidity in the initial and boundary conditions is increased by 10, 20 and 30% (see Section 2.2.1); the red bars when temperature is increased by 1 and 2ºC.

It is worth to note that the events that produced the largest floods do not react strongly to the increased temperature or specific humidity in the affected catchments. Rainfall amounts hardly increased in the Schächen, Lütschine and Dischma in 2005, in the Saltina in 2000 or in the Suze in 2007 when increasing the initial and boundary parameters. It seems that they are already near their optimum in terms of producing maximum precipitation for that specific meteorological situation. In less affected catchments, rainfall amounts can react strongly, like in the Schächen, Hinterrhein and Dischma in October 2000 or in the Suze in August 2005.

The December 1991 event is special. It was included, because it produced the largest flood on record in the Suze. It was found that it produced the largest observed precipitation the Schächen, Dischma and Lütschine, much larger than in the Suze (Piaget, 2015). However, in these catchments, it passed unnoticed, because it produced mainly snow. This huge event occurred in winter from cold air and produced only moderate intensities. Due to the limited sensitivity to humidity and temperature changes, it seems unlikely that a large share of snow could be transformed to liquid precipitation. This event was therefore not considered further for the hydrological simulations.

4.2.2 Events used for extrapolation

The August 2005 event showed the highest sensitivity to changes in humidity and temperature boundary conditions in the Suze (Fig. 2.8). The sensitivity experiments produce rainfall amounts that exceed the ones during the largest recent floods of the Suze observed (e.g. in December 1991). Because the Suze has a limited capacity through Biel, rain events as indicated by the August 2005 sensitivity experiments would be catastrophic. Additional simulations about the magnitude of potential floods would be desirable. However, further research would be required to better define runoff formation in the large karstic areas in the catchment.

The October 2000 event reacted strongest to increases in specific humidity in many catchments. Rainfall amounts more than doubled in the Schächen, Hinterrhein and Dischma (Fig. 2.9). This scenario was used to perform QArea+ simulations in the Hinterrhein and Dischma. In the Schächen, the August 2005 was used, as it was more voluminous than the October 2000 realization. The results are discussed in the Section 4.2.3.

4.2.3 Extrapolated flood peaks

In Table 4.1, the scenario simulations with QArea+ are confronted with the largest flood peaks on record. The scenario peak is 34% higher than the 2005 peak in the Schächen: this increase is proportional with the increase in precipitation. In the Dischma, precipitation increases by about a factor of 3 and results in a peak increase of 26%. Because no meaningful COSMO-2 simulation for the 1987 and 1988 events were possible, for the Hinterrhein the 2000 scenario maximized to 350 mm was applied. A decrease of 43% resulted for the peak flow in comparison with the 1987 event. This peak corresponds only to a 5 to 10 year flood (Fig. 4.9).

These results reflect the differences in hydrologic behavior. The rainfall in the Schächen 2005 was very large and of long duration so that large areas of the catchment contributed to runoff. The increase of

30% in the scenario only moderately intensified runoff formation. Therefore, the increase was proportional to the increase in rainfall.

The Dischma catchment is well shielded due to its topographic situation. For this reason, only moderate rainfall amounts were observed until now, even during "extreme" events. In absolute terms, the scenario 2000 rainfall was only moderate in absolute terms and did not exceed the storage capacities. The duration of the scenario event was much longer than the actual event, so that the average intensity was lower, leading only in a moderate increase in peak flow.

According to the COSMO-2 simulations, larger events than observed until today are possible in the Dischma catchment, although not with magnitudes comparable to other catchments. However, the probability of a spectacular increase in runoff is minor.

The largest floods in the Hinterrhein are caused by high intensity rainfalls that fall on fast reacting areas. Although the amount of the 2000 scenario rainfall is impressive, its moderate intensity produced only a minor flood. The extrapolation to extreme events has to be based on high intensity rainfalls, like 1988. Unfortunately, data limitations prevent us to perform successful COSMO-2 simulations for this event and, as a rough guess, an increase of the 1988 intensities of 30% was used in Table 4.1.

Which return periods should be assigned to the maximized events? The base events produced the largest events on record in the catchments. It was at least a 100 year event in the Schächen, according to the historical studies. In the Hinterrhein and Dischma, they are above 50 year events. The probability of occurrence of the maximized events is definitely smaller; it can be assumed that their return period lies between 200 and 500 years (Fig. 4.9).

Based on the presented meteorological and hydrological models, the floods with higher return periods are behaving according to the usual flood frequency extrapolation in the Hinterrhein and the Dischma and slightly stronger in the Schächen. No larger jumps are foreseeable in these catchments.
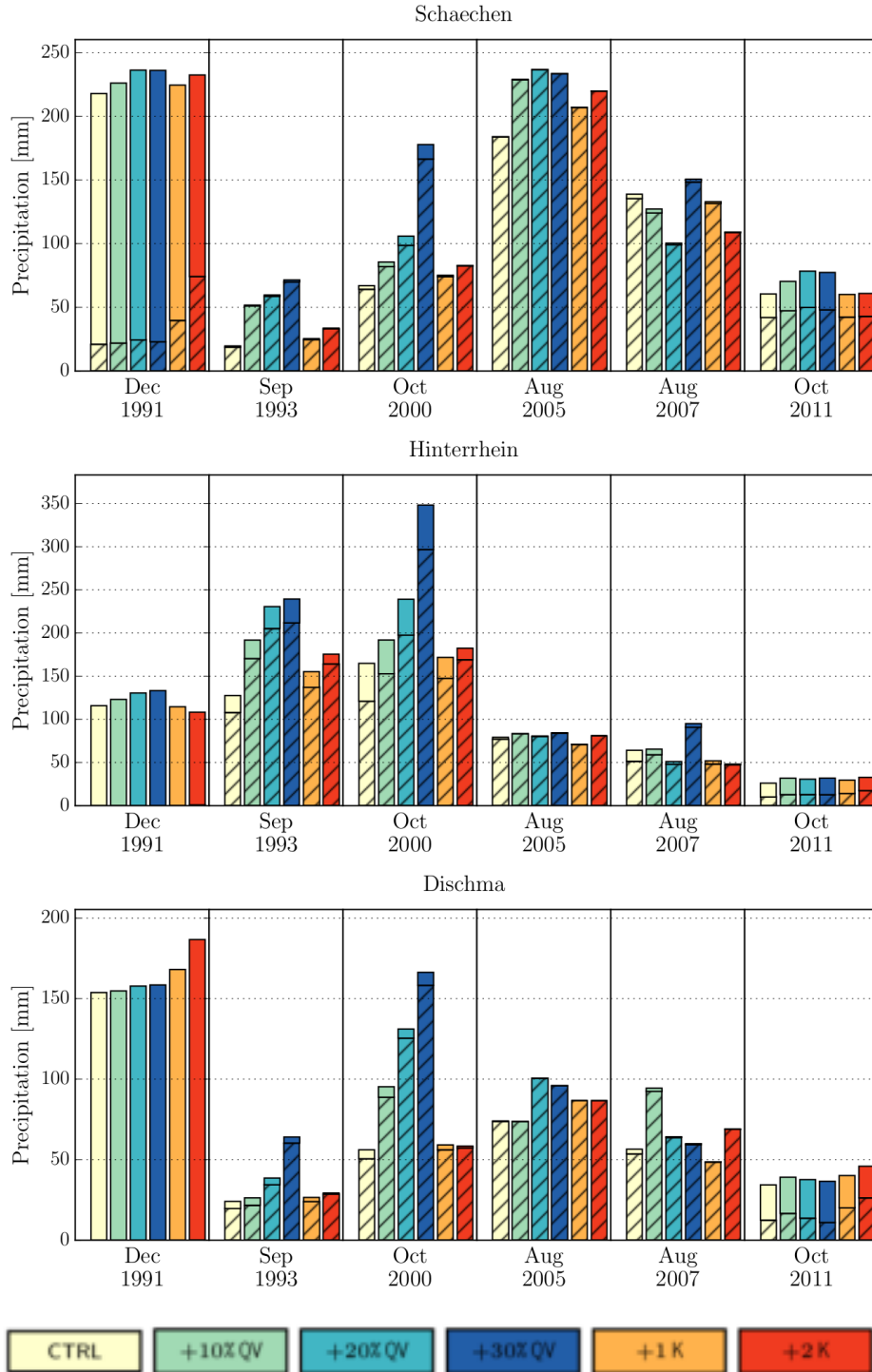
Figure 4.7: Areal average precipitation produced in the COSMO-2 control simulation and scenarios for six events in the Schächen, Hinterrhein and Dischma catchments (different y-axis scales). Precipitation totals are 72-hour sums, except for the October 2011 event, for which only 36 hours could be meaningfully simulated. The rainfall fraction is indicated with hatching (stripes), the colors present the scenario type: 10, 20, or 30% increase in specific humidity (QV) and 1 or 2 degrees Kelvin (K) higher temperatures.
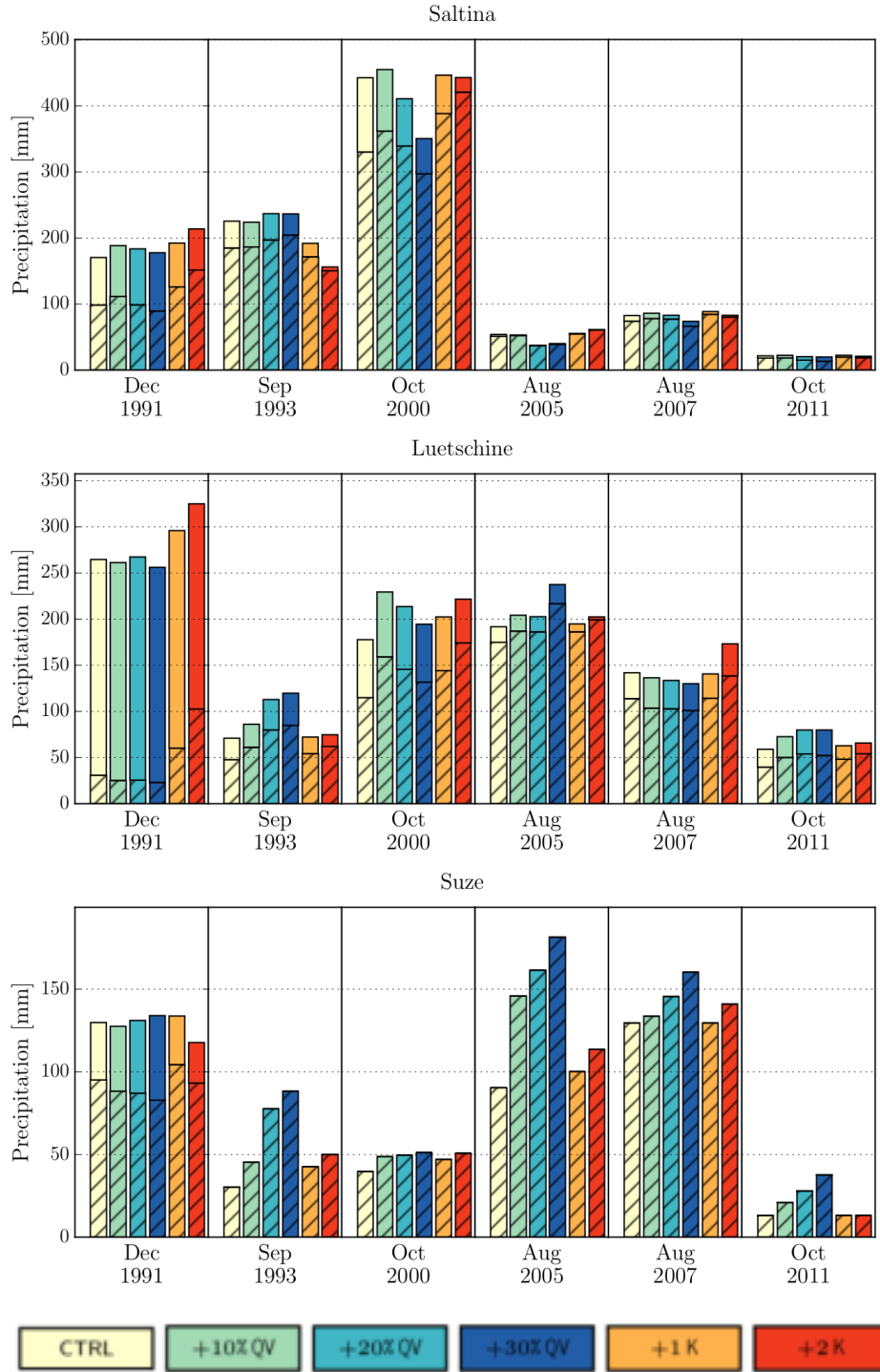
Figure 4.8: Areal average precipitation produced in the COSMO-2 control simulation and scenarios for six events in the Saltina, Luetschine, and Suze catchments. Details as in Fig. 4.7.
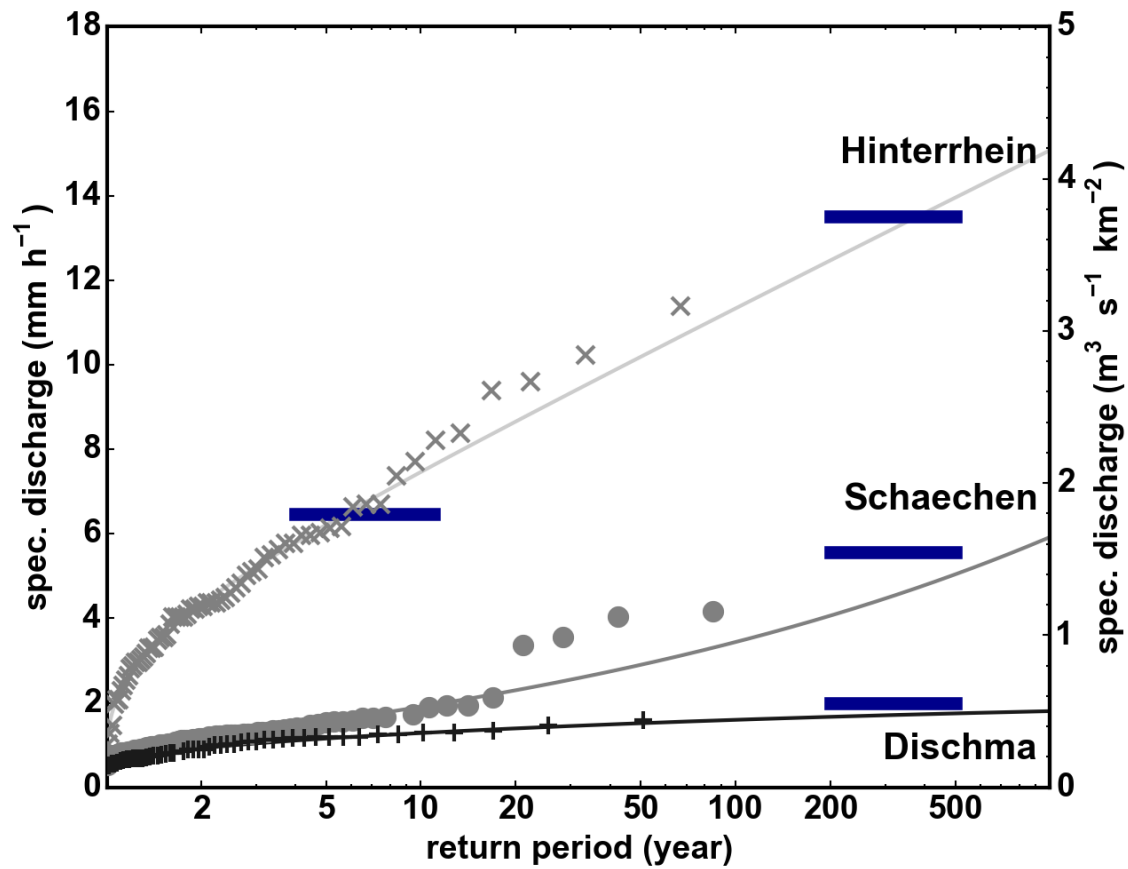
Figure 4.9: Flood frequency analyses of the Hinterrhein, Schächen and Dischma, based on measured yearly maximum floods, complemented with the extreme flood estimates based on the COSMO-2 sensitivity experiments (blue bars, values correspond to the flood peaks listed in Table 4.1).

Table 4.1. Floods peaks estimated with QAREA[+], from rainfall scenarios derived from the COSMO-2 sensitivity experiments. Either the rainfall produced by COSMO-2 was used directly (P_{COSMO}), or an observed rainfall (P_{obs}) was modified to match the average increase in intensity that a representative extreme COSMO-2 scenario projected (e.g., a 30% increase in specific humidity, "qv+30%"). The simulated flood peak, $Q_{peak,scen}$, is then compared to the largest flood peak in the measured record of that catchment, Q_{max}.

	Q_{max} (m³/s)	scenario	$Q_{peak, scen}$ (m³/s)	diff. f. Q_{max}
Schaechen (108 km²)	125 (Aug 2005)	$P_{COSMO-2}$ Aug 2005 with *qv*+30%	167.5	34%
Dischma (43.3 km²)	19 (July 1975)	$P_{COSMO-2}$ Oct 2000 with *qv*+30% (*3.2 x more P*)	24.1	26%
Hinterrhein (54.2 km²)	170 (July 1987)	$P_{COSMO-2}$ Oct 2000 with *qv*+30% (*2.5 x more P*)	96.4	-43%
	170 (July 1987)	P_{obs} Aug 1988 +30% (until Q_{peak})*	201.6	19%

* typical increase of the event's local PMP (e.g., August 2005 in the Schächen and October 2000 in the Saltina).

5   Conclusions and experiences

Extreme floods occur unexpectedly. Existing procedures can predict catchment reactions in the extrapolation range only in very general terms. In this project, advanced meteorological and hydrological models, based on improved understanding of relevant processes, have been combined to investigate reactions of Alpine rivers to physically plausible precipitation events larger than the ones observed until now.

This approach requires large, high quality data sets as input to the simulations. The following limitations were encountered:

It was realized that meteorological data before 1990 did not allow performing COSMO-2 simulations with the required accuracy. Simulated rainfall fields from earlier floods, e.g. 1987, deviated too much from observations to be useful. This drawback was partly compensated by the considerable number of large impact floods that occurred since then.

Efforts were made to classify large precipitation events by their moisture sources, using the 20CR reanalysis data set going back to 1871. If successful, such an analysis could have helped to estimate frequencies of defined meteorological situations. However, the quality of the 20CR data set was not sufficient: the farther back, the less pronounced became differences in moisture uptakes and an assessment of the frequencies of different types of events was not possible.

Therefore, it was also not possible to make educated guesses of the return periods of the maximized rainfall fields used. However, they are based on the largest known events, the return periods lie well over 100 years.

The COSMO-2 simulations reveal the dynamic evolution of intense precipitation fields and show the close, but complex, relation of topography and precipitation development in detail. Relatively small changes in the boundary conditions can produce surprising effects. They do not just influence the amounts; in certain situations, the whole precipitation field and its time distribution can be shifted (see Fig. 2.9 and discussion). This leads to the conclusion that shifting of precipitation fields from one valley to another or statistically extrapolating rainfall stations to derive extreme rainfalls is a too simple approach to be recommended. For catchments in the center of a precipitation event, like the Saltina in 2000, precipitation amounts might be relatively stable; catchments at the border of expanding events, like in the Schächen, Hinterrhein and Dischma in 2000, might experience severe effects.

The work presented requires detailed knowledge of the significant meteorological and hydrological processes and large efforts in data preparation, field work and computer simulations. But it presents a powerful tool to understand and predict the behavior of catchments in the extrapolation range, a requirement that is becoming ever more important in our situation of intensified use of resources and changing climate.

6 References

BAFU, 2001. Hochwasserschutz an Fliessgewässern, Vollzug Umwelt VU, available at: www.bafu.admin.ch/publikationen/publikation/00804/index.html?lang=de

Ban, N., J. Schmidli, and C. Schär, 2014. Evaluation of the convection-resolving regional climate modeling approach in decade-long simulations. J. Geophys. Res. Atmos., 119, 7889-7907.

Ban, N., J. Schmidli, and C. Schär, 2015. Heavy precipitation in a changing climate: Does short-term summer precipitation increase faster? Geophys. Res. Lett. 42, 2014GL062588, doi: 10.1002/2014GL062588.

Bauer, P., A. Thorpe, and G. Brunet, 2015. The quiet revolution of numerical weather prediction. Nature, 525, 47-55.

Compo, G. P. et al. 2011. The Twentieth Century Reanalysis Project. Quart. J. Roy. Meteorol. Soc., 137, 1–28.

Davolio, S., F. Silvestro, and P. Malguzzi, 2015. Effects of increasing horizontal resolution in a convection-permitting model on flood forecasting: the 2011 dramatic events in Liguria, Italy. J. Hydrometeorol., 16, 1843-1856.

Dee, D. P. et al. 2011. The ERA-Interim reanalysis: configuration and performance of the data assimilation system. Quart. J. Roy. Meteorol. Soc., 137, 553–597.

Dirmeyer, P. A., et al., 2012. Simulating the diurnal cycle of rainfall in global climate models: Resolution versus parametrization. Clim. Dyn., 39, 399-418.

Frei, C., J. H. Christensen, M. Déqué, D. Jacob, R. G. Jones, and P. L. Vidale, 2003. Daily precipitation statistics in regional climate models: Evaluation and intercomparison for the European Alps. J. Geophys. Res., 108, 4124, doi: 10.1029/2002JD002287.

Gerstengarbe, F.-W. and P. C. Werner, 1999. Katalog der Grosswetterlagen Europas (1881 - 1998) nach Paul Hess und Helmuth Brezowsky. 5. verbesserte und ergänzte Auflage, Potsdam und Offenbach a. M., 138 pp., available at: www.pik-potsdam.de/~uwerner/gwl/gwl.pdf

Gobiet, A., S. Kotlarski, M. Beniston, G. Heinrich, J. Rajczak, and M. Stoffel, 2014. 21st century climate change in the European Alps - A review. Sci. Tot. Environment, 493, 1138-1151.

Grams, C. M., H. Binder, S. Pfahl, N. Piaget, and H. Wernli, 2014. Atmospheric processes triggering the central European floods in June 2013. Nat. Hazards Earth Syst. Sci., 14, 1691-1702.

Hegg, C., F. Schmid, and E. Frick, 2002. Hochwasser 2000 – Les crues 2000. Ereignisanalyse / Fallbeispiele. Analyse des événements / Cas exemplaires. Berichte des BWG, Serie Wasser 2. Bern: BWG, p. 250, available at:
www.bafu.admin.ch/publikationen/publikation/00316/index.html?lang=de.

Hohenegger, C., A. Walser, W. Langhans, and C. Schär, 2008. Cloud-resolving ensemble simulations of the August 2005 Alpine flood. Quart. J. Roy. Meteorol. Soc., 134, 889-904.

Huth, R., C. Beck, A. Philipp, M. Demuzere, Z. Ustrnul, M. Cahynova, J. Kysely, and O. E. Tveito, 2008. Classification of atmospheric circulation patterns - recent advances and applications, Ann. N. Y. Acad. Sci., 1146, 105-152, doi:10/1196annals.1446.019.

Hybest GmbH, ISSKA, Scherrer AG, & Soilcom GmbH, 2013. Analyse der Gefährdung Biels durch Hochwasser der Schüss, Im Auftrag des Tiefbauamtes des Kantons Bern.

IPCC, 2013: Climate Change 2013: The Physical Science Basis. Contribution of Working Group I to the 5th Assessment Report of the Intergovernmental Panel on Climate Change [Stocker, T. F., D. Qin, G.-K. Plattner, M. Tignor, S. K. Allen, J. Boschung, A. Nauels, Y. Xia, V. Bex, and P. M. Midgley (eds.)]. Cambridge University Press, Cambridge, United Kingdom and New York, NY, USA, 1535 pp.

Kljun, N., M. Sprenger, and C. Schär, 2001. Frontal modification and lee cyclogenesis in the Alps: A case study using the ALPEX reanalysis data set. Meteorol. Atmos. Phys., 78, 89-105.

Kotlarski, S., et al., 2014. Regional climate modelling on European scales: A joint standard evaluation of the EURO-CORDEX RCM ensemble. Geosci. Model Dev., 7, 1297-1333.

Kröner, N. S. Kotlarski, E. Fischer, D. Lüthi, E. Zubler, and C. Schär, 2016. Separating climate change signals into thermodynamic, lapse-rate and circulation effects: Theory and application to the European summer climate. Clim. Dyn., in press.

Markart, G., B. Kohl, B. Sotier, T. Schauer, G. Nunza, and R. Stern, 2004. Provisorische Geländeanleitung Zur Abschätzung Des Oberflächenabflussbeiwertes Auf Alpinen Boden-/Vegetations- Einheiten Bei Konvektiven Starkregen (Version 1.0). Wien: Bundesamt und Forschungszentrum für Wald, available at: bfw.ac.at/rz/bfwcms.web?dok=4343.

MeteoSwiss, 2006. Starkniederschlagsereignis August 2005. Arbeitsberichte der MeteoSchweiz, 211, 63 pp.

Naef, F., and Ch. Lehmann, 2012. Massgebende Hochwasser der Lütschine - unter Berücksichtigung der Häufung der Hochwasser seit dem Jahr 2000, In Auftrag der Tiefbauamtes des Kantons Bern.

Paulat, M., C. Frei, M. Hagen, and H. Wernli, 2008. A gridded dataset of hourly precipitation in Germany: its construction, climatology and application. Meteorol. Z., 17, 719-732.

Piaget, N., 2015. Meteorological characteristics of extreme precipitation and floods in Switzerland. PhD thesis ETH Zürich, No. 22702, 226 pp.

Piaget, N., P. Froidevaux, P. Giannakaki, F. Gierth, O. Martius, M. Riemer, G. Wolf, and C. M. Grams, 2015. Dynamics of a local Alpine flooding event in October 2011: moisture source and large-scale circulation. Quart. J. Roy. Meteorol. Soc., 141, 1922-1937.

Ramos, A. M., M. Sprenger, H. Wernli, A. M. Durán-Quesada, M. N. Lorenzo, and L. Gimeno, 2014. A new circulation type classification based upon Lagrangian air trajectories. Front. Earth Sci., 2, 29, doi:10.3389/feart.2014.00029.

Rotunno, R., and R. A. Houze, 2007. Lessons on orographic precipitation from the Mesoscale Alpine Programme. Quart. J. Roy. Meteorol. Soc., 133, 811-830.

Schär, C., C. Frei, D. Lüthi, and H. C. Davies, 1996. Surrogate climate change scenarios for regional climate models. Geophys. Res. Letters, 23, 669-672.

Scherrer AG, 2007. Hydrologische Grundlagen des Schächen für den Hochwasserschutz des Urner Talbodens und das Generelle Projekt Schächen; Auftraggeber: Amt für Tiefbau des Kantons Uri. Tech. Rep., Scherrer AG, Reinach, Switzerland.

Scherrer, S., 1996. Abflussbildung bei Starkniederschlägen - Identifikation von Abflussprozessen mittels künstlicher Niederschläge. PhD Thesis, ETH Zürich, Zürich. doi:10.3929/ethz-a-001735502

Scherrer, S., and F. Naef, 2003. A decision scheme to indicate dominant flow processes on temperate grassland. Hydrol. Process., 17, 391-401. doi:10.1002/hyp.1131

Scherrer, S., F. Naef, A. O. Faeh, and I. Cordery, 2007. Formation of runoff at the hillslope scale during intense precipitation. Hydrol. Earth Syst. Sci., 11(2), 907-922. doi:10.5194/hess-11-907-2007

Schmocker-Fackel, P., and F. Naef, 2010. Changes in flood frequencies in Switzerland since 1500. Hydrol. Earth Syst. Sci., 14(8), 1581-1594. doi:10.5194/hess-14-1581-2010

Schmocker-Fackel, P., and F. Naef, 2010. More frequent flooding? Changes in flood frequency in Switzerland since 1850. J. Hydrol., 381(1), 1-8. doi:10.1016/j.jhydrol.2009.09.022

Schmocker-Fackel, P., F. Naef, and S. Scherrer, 2007. Identifying runoff processes on the plot and catchment scale. Hydrol. Earth Syst. Sci., 11(7), 891-906. doi:10.5194/hess-11-891-2007

Schüepp, M., 1959. Die Klassifikation der Wetterlagen im Alpengebiet. Geophysica pura et applicata, 44, 242-48.

Schüepp, M., 1996. Typische Wetterlagen und ihre Darstellung im Schweizer Weltatlas. Geographica Helvetica, Nr. 1, 12-19.

Smoorenburg, M., 2015. Flood behavior in alpine catchments examined and predicted from dominant runoff processes. PhD Thesis, ETH Zurich. doi:10.3929/ethz-a-010553048

Sodemann, H., C. Schwierz, and H. Wernli, 2008. Inter-annual variability of Greenland winter precipitation sources: 1. Lagrangian moisture diagnostic and North Atlantic Oscillation influence. J. Geophys. Res., 113, D03107, doi:10.1029/2007JD008503.

Stohl, A., C. Forster, and H. Sodemann, 2008. Remote sources of water vapor forming precipitation on the Norwegian west coast at 60°N – a tale of hurricanes and an atmospheric river. J. Geophys. Res., 113, D05102, doi:10.1029/2007JD009006.

Stucki, P., R. Rickli, S. Brönnimann, O. Martius, H. Wanner, D. Grebner, and J. Luterbacher, 2012. Weather patterns and hydro-climatological precursors of extreme floods in Switzerland since 1868. Meteorol. Z., 21, 531-550.

VAW, 1994a. Die massgebende abflussbildenden Prozesse im Einzugsgebiet der Schüss und ihr Einfluss auf das 100jährliche Hochwasser, Im Auftrag des Tiefbauamtes des Kantons Bern; Bericht Nr. 4071-10, Zürich.

VAW, 1994b. Die Grösse extremer Hochwasser der Saltina – Hydrologische Untersuchungen nach der Hochwasserkatastrophe in Brig vom 24.9.1993, im Auftrag des Krisenstabes Brig-Glis; Bericht Nr. 4080, Zürich.

Winschall, A., S. Pfahl, H. Sodemann, and H. Wernli, 2012. Impact of North Atlantic evaporation hot spots on southern Alpine heavy precipitation events. Quart. J. Roy. Meteorol. Soc., 138, 1245-1258.

Winschall, A., H. Sodemann, S. Pfahl, and H. Wernli, 2014. How important is intensified evaporation for Mediterranean precipitation extremes? J. Geophys. Res. Atmos., 119, 5240-5256, doi:10.1002/2013JD021175.

7   Abbreviations

DP   Deep Percolation
DRP   Dominant Runoff Process
ESMA   Explicit Soil Moisture Accounting
HOF   Hortonian Overland Flow
SOF   Saturation Overland Flow
SSF   Subsurface Stormflow

8   Acknowledgements